2.2. Expression and purification of recombinant αS

Wild-type and deletion mutants of human αS cDNAs were cloned into the pGEX-4T-1 vector (GE Healthcare) to generate glutathione S-transferase fusion protein. The fusion proteins were expressed in *Escherichia coli*. Recombinant αS was purified from the fusion protein by the method described previously [14].

2.3. Oleic acid (OA)-binding assay

OA-binding assay was carried out as previously described with slight modifications [17,19]. Hydroxyalkoxypropyl-Dextran type IV (known as Lipidex 1000, Sigma) was known to bind to free FA at 0–4 °C and FA-bound proteins at 37 °C [19]. To collect FA-unbound proteins, recombinant αS proteins purified from *E. coli* were incubated for 30 min with 5% Lipidex 1000 at 37 °C. After centrifugation at 20000 × *g* for 5 min, the supernatant containing FA-unbound αS was recovered and stored at −80 °C. To determine the binding of αS to OA, 5 μM αS protein was incubated with various amounts of [^{14}C] OA (Moravek Biochemicals, 54 mCi/mmol) in 100 μl of phosphate-buffered saline (PBS; 100 mM phosphate, pH 7.4, 150 mM NaCl) for 1 h at room temperature. The mixture was kept on ice for 10 min, and 10 μl of 50% (v/v) Lipidex 1000 was added. The mixture was incubated for 10 min on ice. After centrifugation at 15000 × *g* for 5 min, protein-bound [^{14}C] OA in the supernatant was measured by scintillation counting.

2.4. In vitro oligomerization of αS

One micromolar recombinant αS proteins in PBS were incubated at 37 °C for 12 h with or without α-linolenic acid (ALA, Sigma) of indicated concentrations [14]. Samples (100 ng protein) were analyzed by immunoblotting using anti-αS monoclonal antibody (Syn-1, which recognizes residues 91–99 of human αS; BD Transduction Laboratories) [20].

2.5. Cell culture and transfection

Human embryonic kidney (HEK) 293 cells were maintained in Dulbecco's modified Eagle's medium (Invitrogen) supplemented with 10% fetal bovine serum. HEK293 cells were transfected with αS cDNAs using Lipofectamine Plus reagents (Invitrogen), according to the manufacturer's protocol.

2.6. PUFA-induced αS oligomerization in the cells

For the PUFA-induced αS oligomerization, the transfectants were recovered at 32 h after transfection, and the cells were further incubated with serum-free medium containing 500 μM ALA and 100 μM FA-free bovine serum albumin (BSA, Sigma) for 16 h [14,18].

2.7. PUFA-induced oligomerization of phosphorylated αS in the cells

HEK293 cells were transiently co-transfected with GRK5 cDNA and either wild-type or mutant αS cDNA [14]. Twenty-four hours after the transfection, 20 nM okadaic acid (Wako) was added to the culture and the cells were incubated for 16 h. The cells were further incubated for 9 h in fresh serum-free medium containing ALA/BSA complexes and okadaic acid and the cell lystaes were analyzed by immunoblotting [14].

2.8. Protein fractionation and immunoblotting

Transfectants of HEK293 cells were suspended in homogenization buffer [20 mM HEPES, pH 7.4, 1 mM $MgCl_2$, 0.32 M sucrose, 43 mM 2-mercaptoethanol, 1 × protease inhibitor cocktail (RocheDiagnostic), 20 mM NaF, 1 mM Na_3VO_4] and were disrupted by brief sonication [14,17]. Samples were sequentially centrifuged at 8000 × *g* for 15 min and at 370000 × *g* for 1 h. The resultant supernatant was recovered and stored as the cytosol fraction. The post-370000 × *g* pellet was disrupted by sonication in homogenization buffer containing 1% Nonidet P-40, 1% sodium deoxycholate and 0.1% SDS, and the homogenates were incubated on ice for 30 min. After centrifugation at 12000 × *g* for 30 min, the supernatant was stored as the pellet fraction. Since the detection of lipid-associated αS oligomers by immunoblotting requires delipidation procedures, we treated the cytosol fractions at 60 °C for 16 h for delipidation prior to gel-loading. The effect of the delipidation for detection of αS oligomers was described previously [14,17,18].

Protein samples were denatured by boiling for 5 min in Laemmli's sample buffer containing 2.5% 2-mercaptoethanol. Immunoblotting was performed as described previously [14]. The transferred membrane was probed with the antibodies as follows: αS specific, Syn-1, LB509 (monoclonal IgG, which recognizes residues 115–122 of αS; Zymed) [21] and 211 (monoclonal IgG, which recognizes residues 121–125 of αS; Sigma) [22]; phosphorylated αS at Ser129 specific, psyn#64 (monoclonal IgG; Wako) [23]; β-actin (Sigma); or superoxide dismutase 1 (SOD1, Stressgen). Bands were visualized by enhanced chemiluminescence (ECL) or ECL plus (GE Healthcare). Relative intensities of detected bands were scanned and quantified with NIH Image J, version 1.33 or Quantity one (Bio-Rad) software.

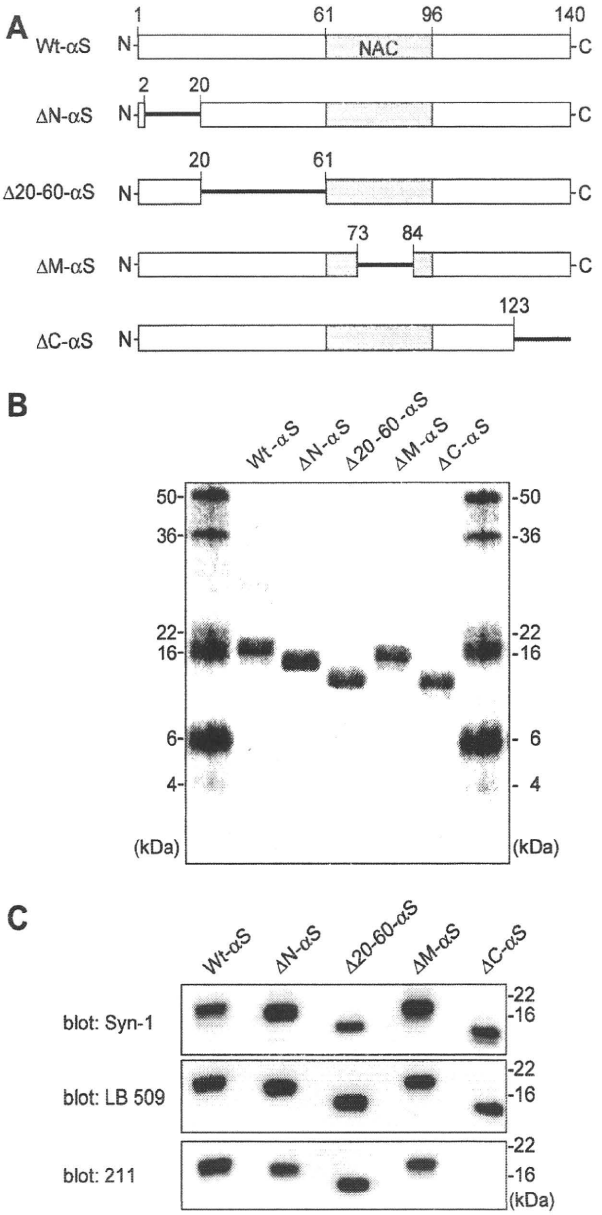

Fig. 1. αS deletion mutants. (A) Schematic diagrams of wild-type αS (Wt-αS) and αS deletion mutants. (B) The purity and electrophoretic pattern of recombinant αS mutants. Recombinant proteins (2 μg) were analyzed by SDS–PAGE using 15% polyacrylamide gel. The gel was stained with Coomassie brilliant blue R-250. (C) Recombinant αS proteins (100 ng) were loaded to the 12.5% polyacrylamide gel and analyzed by immunoblotting using three different monoclonal antibodies. Monoclonal antibodies Syn-1, LB509 and 211 recognize residues 91–95, 115–122 and 121–125, respectively.

3. Results

3.1. Mapping of the FA-binding region of αS

To determine the FA-binding region(s) in the αS molecules, we prepared recombinant wild-type and four deletion mutants of αS protein (Fig. 1A). The first mutant lacks the N-terminal region homologous to the FA-binding motif of FABP (ΔN-αS, residues 2–19) [17]. The second mutant lacks the region between the N-terminal homologous region and the non-amyloid β-protein component (NAC) (Δ20–60-αS, residues 20–60). The third mutant lacks the fibrillization core of the NAC (ΔM-αS, residues 73–83) [24]. The forth mutant lacks the C-terminal region homologous to the FA-binding motif of FABP (ΔC-αS, residues 123–140) [17] (Fig. 1A). Purity of the recombinant proteins was >95%, as determined by SDS–PAGE (Fig. 1B). As shown in Fig. 1B, the mobilities of ΔN-αS, Δ20–60-αS and ΔM-αS monomers corresponded to those expected from the length of deleted amino acids, however, ΔC-αS migrated much faster than the position predicted from its molecular size. We could not elucidate the reason why ΔC-αS had high electrophoretic mobility. To confirm the amino acid sequence lacking in the product of ΔC-αS, we performed immunoblots

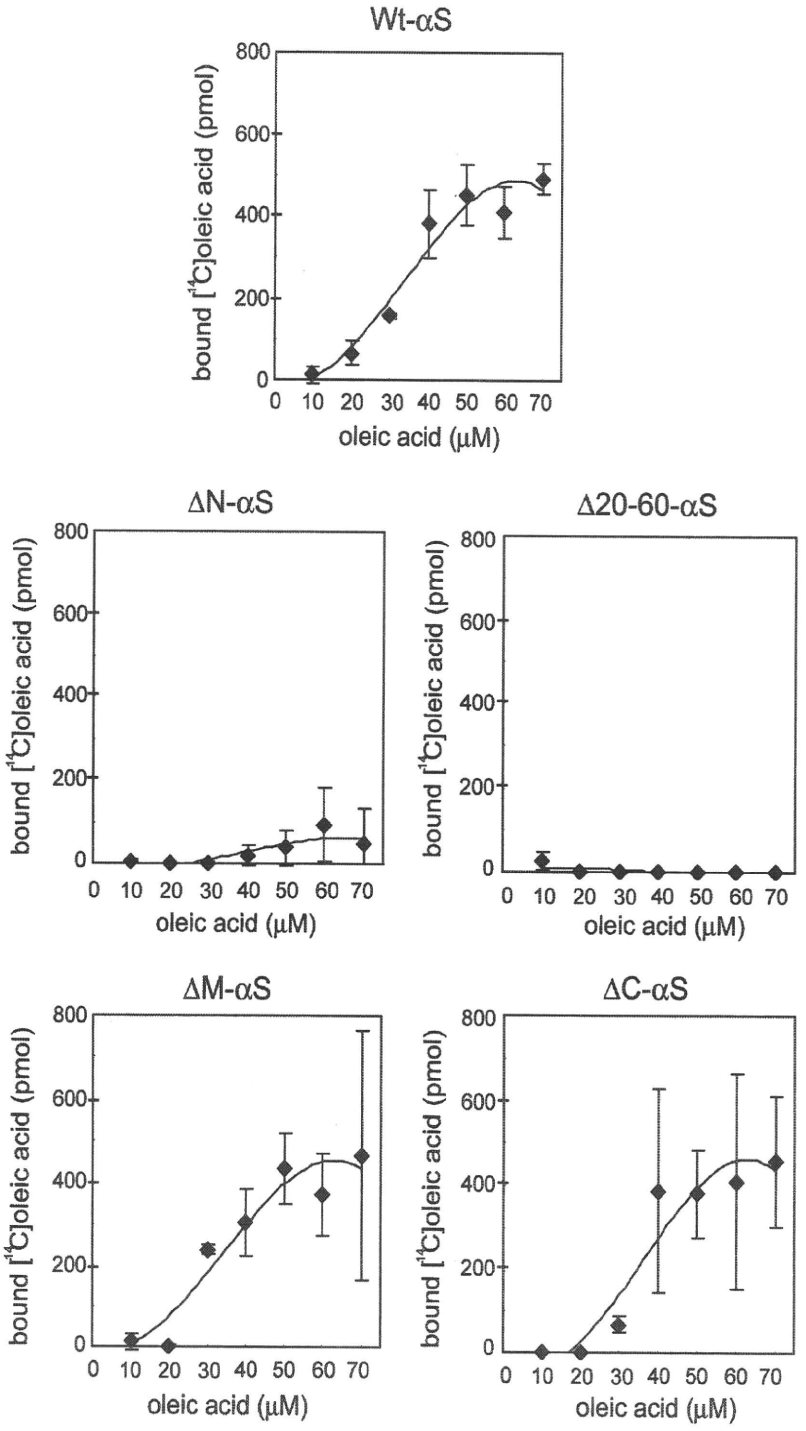

Fig. 2. Analysis of the FA-binding region of αS. Purified αS protein (5 μM) was incubated with [^{14}C] OA of various concentrations. Protein-bound [^{14}C] OA was separated from free [^{14}C] OA by using Lipidex 1000 (see Section 2). Data points represent means ± S.D. (n = 3).

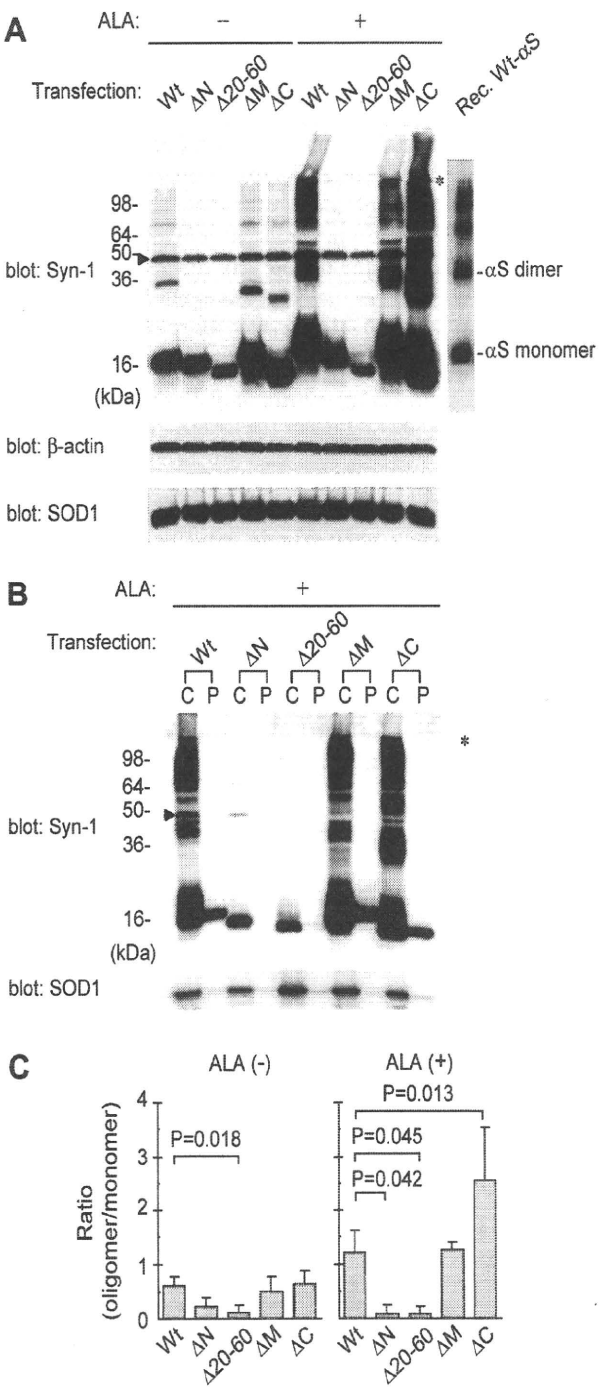

Fig. 3. Analysis of the αS region required for PUFA-induced oligomerization. (A) αS deletion mutants differentially affect ALA-induced αS oligomerization. HEK293 cells expressing either wild-type αS or one of the deletion mutants were incubated for 16 h in serum-free medium containing BSA (100 μM) or ALA/BSA complexes (500/100 μM). Cytosol fractions (30 μg protein) were heat-treated as described in the Materials and methods and analyzed by immunoblotting. αS oligomers from ALA-treated recombinant αS protein (Rec.) are also shown. The asterisk indicates the interface of resolving and stacking gels; the arrowhead points to a non-specific band (~47 kDa) by Syn-1 antibody. For loading control, same amounts of non-heat-treated samples were immunoblotted with anti-β-actin and anti-SOD1 antibodies. (B) Distribution of αS proteins in cytosol and pellet fractions. HEK293 cells expressing either wild-type αS or one of the deletion mutants were incubated for 16 h in serum-free medium containing ALA/BSA complexes. Cytosol fractions (20 μg protein, lanes C) and pellet fractions (20 μg protein, lanes P) were heat-treated and analyzed by immunoblotting. For loading control, same amounts of non-heat-treated samples were immunoblotted with anti-SOD1 antibody. (C) Quantitative analysis of PUFA-induced αS oligomerization in deletion mutants. Relative ratio of the band intensity of oligomers (subtracting the non-specific 47 kDa band from total oligomers above 37 kDa) to that of monomers is shown. Data represent means ± S.D. ($n = 5$ Wt-αS, ΔM-αS, and ΔC-αS; $n = 3$ ΔM-αS). The *P*-values were estimated by ANOVA with post hoc Scheffe test.

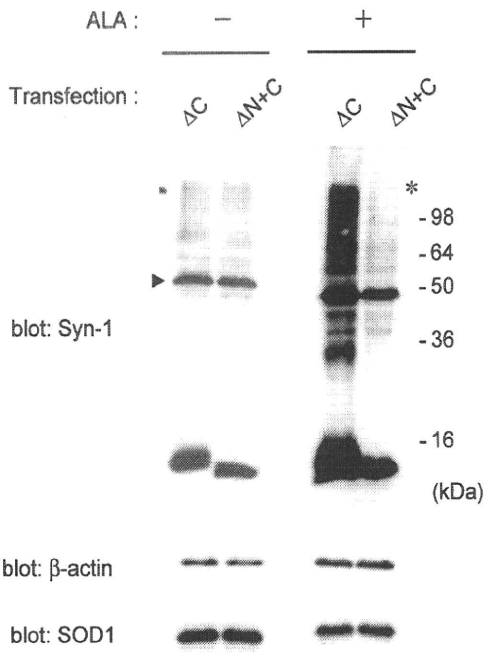

Fig. 4. The N-terminal FA-binding region is required for the accelerating effect of C-terminally truncated αS on the PUFA-induced oligomerization. HEK293 cells expressing either ΔC-αS (lacking residues 123–140) or ΔN+C-αS (lacking residues 2–19 and 123–140) were incubated for 16 h in serum-free medium containing BSA (100 μM) or ALA/BSA complexes (500/100 μM). Cytosol fractions (30 μg protein) were heat-treated and analyzed by immunoblotting with Syn-1. For loading control, same amounts of non-heat-treated samples were immunoblotted with anti-β-actin and anti-SOD1 antibodies. The asterisk indicates the interface of resolving and stacking gels; the arrowhead points to the non-specific band by Syn-1.

with 211 and LB509 monoclonal antibodies, which recognize residues 121–125 and 115–122 of αS, respectively. As expected, the product of ΔC-αS reacted with LB509, but not with 211 (Fig. 1C and Supplemental Fig. 1).

We determined the binding of [^{14}C] OA to the deletion mutants by the Lipidex assay [17,19]. Dose-dependent binding of [^{14}C] OA was observed when a constant amount (5 μM) of purified recombinant Wt-αS was incubated with [^{14}C] OA of various concentrations (10–70 μM) (Fig. 2). Among the deletion mutants, both ΔM-αS and ΔC-αS bound OA in a dose-dependent manner. In contrast, both ΔN-αS and Δ20–60-αS failed to bind a significant amount of [^{14}C] OA under the same experimental conditions (Fig. 2).

3.2. Role of the FA-binding region of αS in the PUFA-induced oligomerization

In order to determine whether the binding of PUFA to αS enhances the oligomerization of αS, we assessed the formation of soluble oligomers in the cells transfected with one of the deletion mutants in the presence or absence of ALA. In the cytosol fraction of the cells expressing Wt-αS, ΔM-αS, or

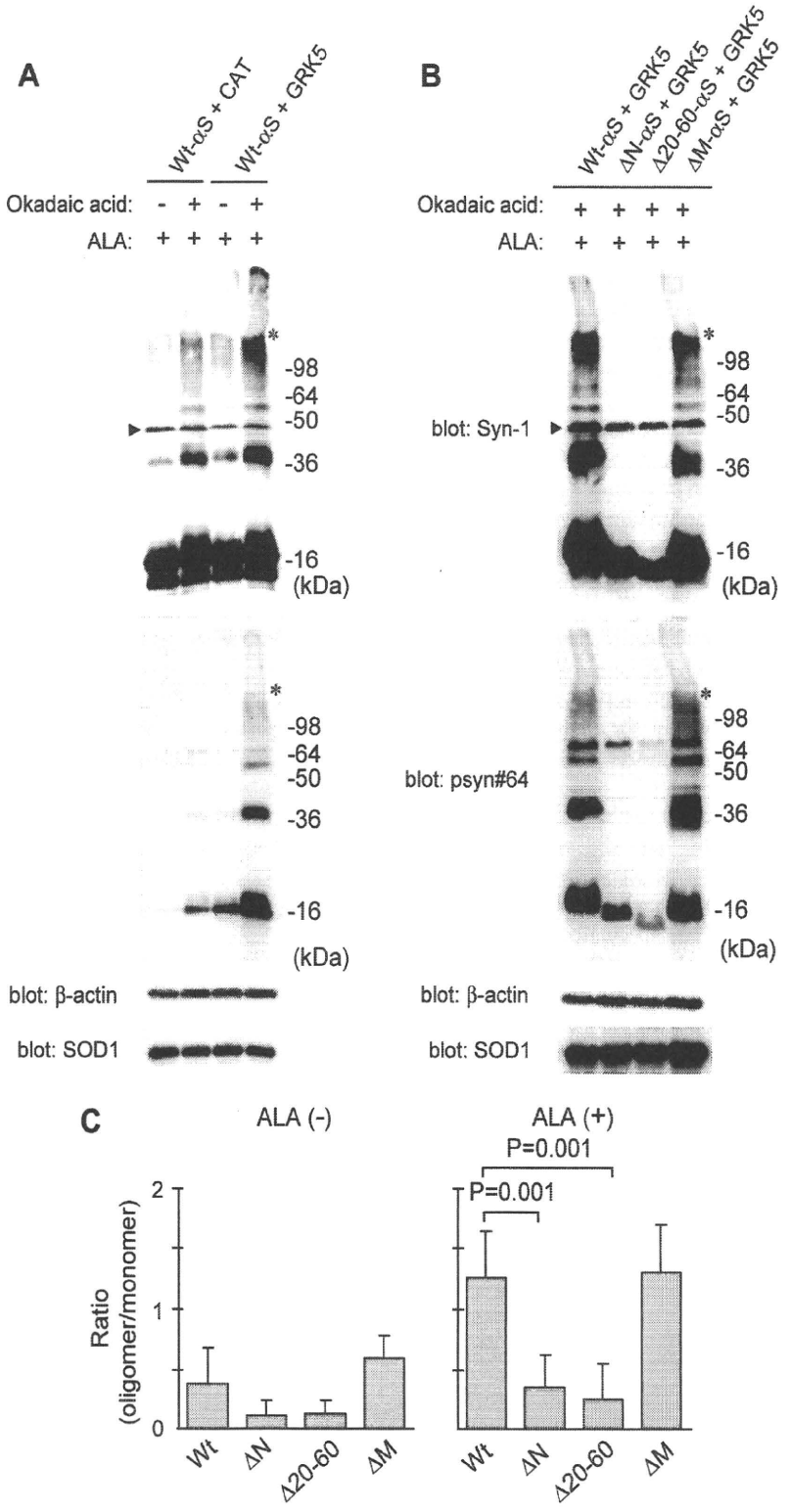

Fig. 5. The N-terminal FA-binding region is required for the accelerating effect of phosphorylation of Ser129 in αS on the PUFA-induced oligomerization. (A) HEK293 cells co-expressing αS and either chloramphenicol acetyltransferase (CAT) or GRK5 were incubated for 9 h in serum-free medium containing ALA/BSA complexes (500/100 μM) with or without 20 nM okadaic acid. Cytosol fractions (30 μg protein) were heat-treated and analyzed by immunoblotting with Syn-1 and psyn#64. (B) Cells co-expressing GRK5 and each of the deletion mutants were incubated for 9 h in serum-free medium containing ALA/BSA complexes (500/100 μM) and 20 nM okadaic acid. Cytosol fractions (30 μg protein) were heat-treated and analyzed by immunoblotting with Syn-1. For loading control, same amounts of non-heat-treated samples were immunoblotted with anti-β-actin and anti-SOD1 antibodies. Asterisks indicate the interface of resolving and stacking gels; arrowheads point to the non-specific band by Syn-1. (C) Relative ratio of band intensity of oligomers to that of monomers is shown. Data points represent means ± S.D. ($n = 6$). The P-values were estimated by ANOVA with post hoc Scheffe test.

ΔC-αS, the formation of soluble oligomers was enhanced by the treatment with ALA (Fig. 3A). The size distribution of the oligomers of wild-type αS formed by the ALA treatment was comparable to that of recombinant αS oligomers (Fig. 3A). As reported by Sharon et al. [18], smear pattern in the background and gel-excluded immunoreactive material

were obtained in the cells expressing Wt-αS in response to the ALA treatment. The smear pattern may represent aggregated αS that is partially SDS-soluble. The gel-excluded material may represent the species that are SDS-insoluble. In the cytosol fractions of the cells expressing ΔM-αS or ΔC-αS, the smear pattern and gel-excluded material were also observed. In the cytosol fractions of the cells expressing either ΔN-αS or Δ20–60-αS, however, none of the αS oligomers, smear pattern nor gel-excluded material was formed in the presence of ALA (Fig. 3A). The expression of ΔN-αS and Δ20–60-αS was lower than that of the other counterparts. To exclude the possibility that the N-terminal truncation of ΔN-αS and Δ20–60-αS resulted in the formation of insoluble proteins, we assessed whether or not the products of the mutants were present in the pellet fractions of ALA-treated cells. In the pellet fraction of the cells expressing either Wt-αS, ΔM-αS, or ΔC-αS, small amounts of αS monomers, but none of the αS oligomers, smear pattern nor gel-excluded material, were detectable (Fig. 3B). In the pellet fraction of the cells expressing either ΔN-αS or Δ20–60-αS, neither the αS monomer nor oligomer was detectable (Fig. 3B). To correct the difference in expression levels of αS among the transfectants in the cytosol fractions, we determined the relative ratio of the band intensity of the oligomers to that of monomers. The proportion of the soluble oligomers of ΔN-αS or Δ20–60-αS to the monomers in the presence of ALA was lower than the proportion of the oligomers of Wt-αS (Fig. 3C).

In the cells overexpressing Wt-αS, ΔM-αS, or ΔC-αS, the αS monomer in the cytosol fractions markedly increased after exposure to ALA (Fig. 3A). The same phenomenon has been previously described [18]. Apparent increase in the monomers of αS after the PUFA treatment was speculated to be due to conformational changes of the molecules that enhance antibody recognition [18].

In order to assess whether the binding of PUFA to αS induces the αS oligomerization, each of the recombinant proteins of wild-type and deletion mutants was incubated with ALA for 12 h at 37 °C. Analysis of recombinant Wt-αS, ΔM-αS, or ΔC-αS after incubation with ALA showed that ALA enhanced the formation of oligomers (Supplemental Fig. 2). It was noted that the proportion of oligomers of ΔN-αS or Δ20–60-αS was significantly lower than that of Wt-αS (Supplemental Fig. 2).

3.3. Requirement of the FA-binding region for the acceleration of αS oligomerization by C-terminal truncation and phosphorylation of Ser129

As shown in Fig. 3A and C, ΔC-αS formed higher levels of soluble oligomers in the presence of ALA than Wt-αS, indicating that the C-terminal truncation of αS accelerated the formation of oligomers in the presence of PUFA. To investigate possible roles of the C-terminal region of αS in the PUFA-induced oligomerization, we determined the oligomerization of the deletion mutant which lacks both the N-terminal and C-terminal regions (ΔN+C-αS, lacking residues 2–19 and 123–140, Supplemental Fig. 1). The cells expressing ΔN+C-αS failed to form soluble αS oligomers in the presence of ALA, although comparable amounts of αS monomers were found in the ΔN+C-αS and the ΔC-αS mutants (Fig. 4).

As described in our previous report [14], co-overexpression of αS and GRK5 in HEK293 cells in the presence of okadaic acid resulted in phosphorylation of Ser129 in αS and acceleration of the PUFA-induced formation of soluble αS oligomers, in comparison with the cells overexpressing chloramphenicol acetyltransferase (CAT) (Fig. 5A). To assess possible roles of phosphorylation of Ser129 in the PUFA-induced oligomerization of αS, we analyzed the cells co-transfected with GRK5 and one of the αS deletion mutants. The levels of soluble αS oligomers in the presence of ALA decreased in the cells expressing ΔN-αS or Δ20–60-αS, as compared with the cells expressing Wt-αS or ΔM-αS (Fig. 5B). When measured relative ratio of the band intensity of oligomers to that of monomers, the formation of soluble oligomers of ΔN-αS or Δ20–60-αS in the presence of ALA was much less than that of Wt-αS (Fig. 5C).

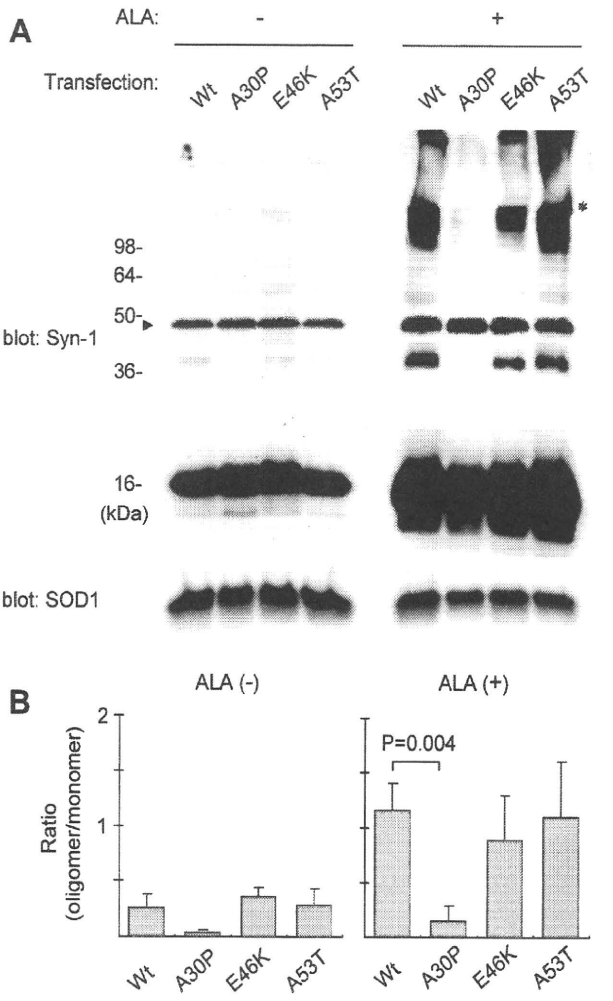

Fig. 6. The effect of familial PD-linked mutations of αS on the PUFA-induced oligomerization of αS. (A) HEK293 cells expressing either Wt-αS, A30P-αS, E46K-αS, or A53T-αS were incubated for 8 h in the presence or absence of ALA/BSA complexes (500/100 μM). Cytosol fractions (30 μg protein) were heat-treated and analyzed by immunoblotting with Syn-1. For loading control, same amounts of non-heat-treated samples were immunoblotted with the anti-SOD1 antibody. Asterisks indicate the interface of resolving and stacking gels; arrowheads point to the non-specific band by Syn-1. (B) Relative ratio of band intensity of oligomers to that of monomers is shown. Data represent means ± S.D. ($n = 5$). The P-values were estimated by ANOVA with post hoc Scheffe test.

3.4. PUFA-induced oligomerization of αS with familial PD-linked mutations

We investigated whether αS with familial PD-linked mutations facilitates the PUFA-induced oligomerization using the cells transfected with one of the familial PD-linked αS mutants. The levels of soluble αS oligomers in the presence of ALA were comparable in the cells expressing either E46K-αS, A53T-αS, or Wt-αS (Fig. 6A and B). However, the cells expressing A30P-αS failed to form soluble oligomers of the mutant αS in the presence of ALA (Fig. 6A and B).

4. Discussion

The present study revealed that recombinant αS proteins bound FA through the amino acid residues 2–60 of αS. Of direct relevance to the result is the report that recombinant αS binds phospholipids with acidic head groups through the amino acid residues 1–102 of αS [25]. The N-terminal half of αS consists of seven repeats with an 11-residue periodicity [26]. The 11-residue repeats are a hallmark of the primary structure of apolipoproteins [27]. The 11-residue repeats of apolipoproteins are known to take the conformation of amphipathic α-helix, which is essential for the binding to lipids [27]. As predicted by the structural similarity of αS to apolipoproteins, the N-terminus of αS is shown to form the amphipathic α-helix [26] and bind acidic phospholipids through the amphipathic α-helix [26]. Therefore, it seems that the amphipathic α-helix in the N-terminus of αS is also required for the binding of αS to FA as well as phospholipids. The deletion mutants of αS lacking the residues 2–19 or 20–60 may disrupt the conformation of the amphipathic α-helix in the N-terminus of αS, resulting in the loss of αS binding to FA.

We also investigated whether the N-terminal region of αS is required for the PUFA-induced oligomerization of αS, and found that the αS mutants lacking the residues 2–19 or 20–60 failed to form αS oligomers in the presence of PUFA. This indicates that the N-terminal FA-binding region of αS is also essential for the PUFA-induced oligomerization of the molecules.

Recent biochemical study has shown that most of αS deposited in LB was phosphorylated at Ser129 and that a small proportion of the deposited αS was C-terminally truncated [28]. It has also been reported that the C-terminal truncation [10,15,29] or Ser129 phosphorylation [13,14] facilitates the formation of αS oligomers and aggregates. In the present study, we determined the effect of the C-terminal truncation or Ser129 phosphorylation on the PUFA-induced oligomerization of αS, and found that both of the C-terminal modifications of αS were able to accelerate the formation of αS oligomers induced by PUFA. This accelerating effect was abolished by the deletion of the N-terminus of αS, suggesting that the N-terminus of αS is indispensable for the PUFA-induced oligomerization of αS and that the C-terminus may function as a modifier for the αS oligomerization.

In the present study, it was found that either the E46K or A53T mutation of αS had no apparent effect on the PUFA-induced oligomerization of αS, as compared with wild-type αS. However, the A30P mutant failed to form αS oligomers in the presence of PUFA. The latter observation is in agreement with the report that αS inclusions are not detectable in the transgenic mice with the A30P mutation of the αS gene [30]. It has been reported that the A30P mutation may disrupt the conformation of the N-terminal α-helix of αS, although the E46K or A53T mutation may not [31]. The conformational changes may explain why the A30P mutant lost the ability to bind to PUFA in the present study.

Although the αS oligomerization induced by PUFA has been emphasized to play a crucial role in the pathogenesis of PD [18], the present observation suggests that the PUFA-induced oligomerization of αS may not be essential for the pathogenesis, especially in the familial PD with A30P mutation of the αS gene. Possible explanation for the neurotoxicity by this mutant is that an impaired binding of the A30P mutant to the phospholipids of the membranes [32,33] may lead to the accumulation of this protein in the cytosol, and the excess accumulation of αS in the cytosol may cause the formation of αS oligomers and fibrils in a PUFA-independent manner [11]. Another possibility is that the ability of αS to bind to the membranous structures, such as synaptic vesicles and presynaptic membrane, may be lost by this mutation [32,33], and this may result in an impairment of synaptic function [34,35], eventually leading to neurodegeneration.

In conclusion, we revealed the importance of the N-terminus of wild-type αS in the PUFA-induced oligomerization of αS. This property of αS was lost by the A30P mutation of αS, suggesting that the degeneration of dopaminergic neurons occurs without the process of the PUFA-induced oligomerization of αS in this form of familial PD. Further studies are needed to clarify the mechanism for the oligomerization of αS into fibrils and toxic species of αS. It may provide a clue for the elucidation of a novel therapeutic strategy for PD.

Acknowledgments: This work was supported in part by the 21st Century Center of Excellence (COE) Program (F03), Japan (T.K.) and supported by Grant-in-Aid for Scientific Research (C) (S.A. #19590979).

Appendix A. Supplementary data

Supplementary data associated with this article can be found, in the online version, at doi:10.1016/j.febslet.2008.10.001.

References

[1] Polymeropoulos, M.H. et al. (1997) Mutation in the alpha-synuclein gene identified in families with Parkinson's disease. Science 276, 2045–2047.
[2] Kruger, R. et al. (1998) Ala30Pro mutation in the gene encoding alpha-synuclein in Parkinson's disease. Nat. Genet. 18, 106–108.
[3] Zarranz, J.J. et al. (2004) The new mutation, E46K, of alpha-synuclein causes Parkinson and Lewy body dementia. Ann. Neurol. 55, 164–173.
[4] Singleton, A.B. et al. (2003) Alpha-synuclein locus triplication causes Parkinson's disease. Science 302, 841.
[5] Spillantini, M.G., Schmidt, M.L., Lee, V.M., Trojanowski, J.Q., Jakes, R. and Goedert, M. (1997) Alpha-synuclein in Lewy bodies. Nature 388, 839–840.
[6] Conway, K.A., Harper, J.D. and Lansbury, P.T. (1998) Accelerated in vitro fibril formation by a mutant alpha-synuclein linked to early-onset Parkinson disease. Nat. Med. 4, 1318–1320.
[7] Masliah, E. et al. (2000) Dopaminergic loss and inclusion body formation in alpha-synuclein mice. Implications for neurodegenerative disorders. Science 287, 1265–1269.

[8] Giasson, B.I., Duda, J.E., Quinn, S.M., Zhang, B., Trojanowski, J.Q. and Lee, V.M. (2002) Neuronal alpha-synucleinopathy with severe movement disorder in mice expressing A53T human alpha-synuclein. Neuron 34, 521–533.
[9] Lee, M.K. et al. (2002) Human alpha-synuclein-harboring familial Parkinson's disease-linked Ala-53 –> Thr mutation causes neurodegenerative disease with alpha-synuclein aggregation in transgenic mice. Proc. Natl. Acad. Sci. USA 99, 8968–8973.
[10] Periquet, M., Fulga, T., Myllykangas, L., Schlossmacher, M.G. and Feany, M.B. (2007) Aggregated alpha-synuclein mediates dopaminergic neurotoxicity in vivo. J. Neurosci. 27, 3338–3346.
[11] Lee, V.M. and Trojanowski, J.Q. (2006) Mechanisms of Parkinson's disease linked to pathological alpha-synuclein: new targets for drug discovery. Neuron 52, 33–38.
[12] Paxinou, E. et al. (2001) Induction of alpha-synuclein aggregation by intracellular nitrative insult. J. Neurosci. 21, 8053–8061.
[13] Fujiwara, H. et al. (2002) Alpha-synuclein is phosphorylated in synucleinopathy lesions. Nat. Cell. Biol. 4, 160–164.
[14] Arawaka, S. et al. (2006) The role of G-protein-coupled receptor kinase 5 in pathogenesis of sporadic Parkinson's disease. J. Neurosci. 26, 9227–9238.
[15] Crowther, R.A., Jakes, R., Spillantini, M.G. and Goedert, M. (1998) Synthetic filaments assembled from C-terminally truncated alpha-synuclein. FEBS Lett. 436, 309–312.
[16] Perrin, R.J., Woods, W.S., Clayton, D.F. and George, J.M. (2001) Exposure to long chain polyunsaturated fatty acids triggers rapid multimerization of synucleins. J. Biol. Chem. 276, 41958–41962.
[17] Sharon, R., Goldberg, M.S., Bar-Josef, I., Betensky, R.A., Shen, J. and Selkoe, D.J. (2001) Alpha-synuclein occurs in lipid-rich high molecular weight complexes, binds fatty acids, and shows homology to the fatty acid-binding proteins. Proc. Natl. Acad. Sci. USA 98, 9110–9115.
[18] Sharon, R., Bar-Joseph, I., Frosch, M.P., Walsh, D.M., Hamilton, J.A. and Selkoe, D.J. (2003) The formation of highly soluble oligomers of alpha-synuclein is regulated by fatty acids and enhanced in Parkinson's disease. Neuron 37, 583–595.
[19] Glatz, J.F. and Veerkamp, J.H. (1983) A radiochemical procedure for the assay of fatty acid binding by proteins. Anal. Biochem. 132, 89–95.
[20] Perrin, R.J., Payton, J.E., Barnett, D.H., Wraight, C.L., Woods, W.S., Ye, L. and George, J.M. (2003) Epitope mapping and specificity of the anti-alpha-synuclein monoclonal antibody Syn-1 in mouse brain and cultured cell lines. Neurosci. Lett. 349, 133–135.
[21] Jakes, R., Crowther, R.A., Lee, V.M., Trojanowski, J.Q., Iwatsubo, T. and Goedert, M. (1999) Epitope mapping of LB509, a monoclonal antibody directed against human alpha-synuclein. Neurosci. Lett. 269, 13–16.
[22] Giasson, B.I., Jakes, R., Goedert, M., Duda, J.E., Leight, S., Trojanowski, J.Q. and Lee, V.M. (2000) A panel of epitope-specific antibodies detects protein domains distributed throughout human alpha-synuclein in Lewy bodies of Parkinson's disease. J. Neurosci. Res. 59, 528–533.
[23] Saito, Y. et al. (2003) Accumulation of phosphorylated alpha-synuclein in aging human brain. J. Neuropathol. Exp. Neurol. 62, 644–654.
[24] Kahle, P.J. et al. (2001) Selective insolubility of alpha-synuclein in human Lewy body diseases is recapitulated in a transgenic mouse model. Am. J. Pathol. 159, 2215–2225.
[25] Perrin, R.J., Woods, W.S., Clayton, D.F. and George, J.M. (2000) Interaction of human alpha-synuclein and Parkinson's disease variants with phospholipids. Structural analysis using site-directed mutagenesis. J. Biol. Chem. 275, 34393–34398.
[26] Davidson, W.S., Jonas, A., Clayton, D.F. and George, J.M. (1998) Stabilization of alpha-synuclein secondary structure upon binding to synthetic membranes. J. Biol. Chem. 273, 9443–9449.
[27] Segrest, J.P., Jones, M.K., De Loof, H., Brouillette, C.G., Venkatachalapathi, Y.V. and Anantharamaiah, G.M. (1992) The amphipathic helix in the exchangeable apolipoproteins: a review of secondary structure and function. J. Lipid Res. 33, 141–166.
[28] Anderson, J.P. et al. (2006) Phosphorylation of Ser-129 is the dominant pathological modification of alpha-synuclein in familial and sporadic Lewy body disease. J. Biol. Chem. 281, 29739–29752.
[29] Tofaris, G.K. et al. (2006) Pathological changes in dopaminergic nerve cells of the substantia nigra and olfactory bulb in mice transgenic for truncated human alpha-synuclein(1–120): implications for Lewy body disorders. J. Neurosci. 26, 3942–3950.
[30] Yavich, L. et al. (2005) Locomotor activity and evoked dopamine release are reduced in mice overexpressing A30P-mutated human alpha-synuclein. Neurobiol. Dis. 20, 303–313.
[31] Chandra, S., Chen, X., Rizo, J., Jahn, R. and Sudhof, T.C. (2003) A broken alpha-helix in folded alpha-synuclein. J. Biol. Chem. 278, 15313–15318.
[32] Jensen, P.H., Nielsen, M.S., Jakes, R., Dotti, C.G. and Goedert, M. (1998) Binding of alpha-synuclein to brain vesicles is abolished by familial Parkinson's disease mutation. J. Biol. Chem. 273, 26292–26294.
[33] Jo, E., Fuller, N., Rand, R.P., St. George-Hyslop, P. and Fraser, P.E. (2002) Defective membrane interactions of familial Parkinson's disease mutant A30P alpha-synuclein. J. Mol. Biol. 315, 799–807.
[34] Clayton, D.F. and George, J.M. (1998) The synucleins: a family of proteins involved in synaptic function, plasticity, neurodegeneration and disease. Trends Neurosci. 21, 249–254.
[35] Larsen, K.E. et al. (2006) Alpha-synuclein overexpression in PC12 and chromaffin cells impairs catecholamine release by interfering with a late step in exocytosis. J. Neurosci. 26, 11915–11922.

Heat Shock Proteins as Suppressors of Accumulation of Toxic Prefibrillar Intermediates and Misfolded Proteins in Neurodegenerative Diseases

Shigeki Arawaka*, Youhei Machiya and Takeo Kato

Department of Neurology, Hematology, Metabolism, Endocrinology, and Diabetology, Yamagata University Faculty of Medicine, 2-2-2 Iida-nishi, Yamagata 990-9585, Japan

Abstract: The most characteristic feature of neurodegenerative diseases, including Alzheimer's disease, Parkinson's disease, amyotrophic lateral sclerosis and Huntington's disease, is the occurrence of extra- or intracellular fibrillar aggregates containing misfolded proteins with beta-sheet conformation. These aggregates are composed of distinct proteins in each neurodegenerative disease. However, mutations in genes encoding major constituents of aggregates, such as Abeta, tau, alpha-synuclein, SOD1 and huntingtin, have been identified to causally associate with familial forms of the diseases. Biochemical studies demonstrate that these mutant and some wild-type proteins tend to be misfolded or form aggregates. It has been proposed that these diseases are caused by a common mechanism involving misfolded proteins that trigger a toxic cascade leading to neuronal degeneration. This hypothesis is the basis of the therapeutic potential of heat shock proteins (HSPs), which prevent protein misfolding and aggregation. Transgenic animal models of the diseases have demonstrated that induction or overexpression of HSPs can suppress neuronal dysfunction and degeneration. Do the results promise clinical success for HSP-based therapy in neurodegenerative diseases? Recent findings regarding the pathogenic species generated during fibril formation have highlighted some of the beneficial and problematic aspects of HSP-based therapy. In this review, we focus on the pathogenic role of prefibrillar intermediates, including soluble oligomers and protofibrils, on neurodegeneration, and the relationship between prefibrillar intermediates and the proteins targeted by HSPs. We discuss *in vitro* and *in vivo* experimental data showing that HSPs counteract disease progression by acting as suppressors of toxic prefibrillar intermediates and toxic misfolded proteins in neurodegenerative diseases.

Keywords: Neurodegenerative disease, Alzheimer's disease, Parkinson's disease, Amyotrophic lateral sclerosis, Huntington's disease, Heat shock protein, Soluble oligomer, Protofibril.

INTRODUCTION

A chemical co-inducer of heat shock protein (HSP) expression, arimoclomol, was reported to slow disease progression in a mutant Cu/Zn superoxide dismutase (SOD1) transgenic mouse model of familial amyotrophic lateral sclerosis (ALS) [1, 2]. Arimoclomol is now being tested clinically in patients with ALS [3]. Induction of HSPs is argued to be a promising strategy for therapeutic intervention in not only the small subgroup of familial ALS but also sporadic ALS and other devastating neurodegenerative diseases, such as Alzheimer's disease (AD), Parkinson's disease (PD) and Huntington's disease (HD) [4]. This is because these neurodegenerative disorders have been proposed to be caused by a common mechanism of protein misfolding [5-12]. It is important to elucidate the mechanisms of HSP up-regulation by chemical compounds and to estimate the clinical effects of these compounds on disease progression. However, it is also useful to assess the background concepts in HSP-based treatment, because of recent findings regarding the pathogenesis of fibril formation. This review discusses experimental data that demonstrate the relationship between the toxicity of misfolded proteins and HSP-target proteins in neurodegenerative diseases.

*Address correspondence to this author at the Department of Neuology, Hematology, Metabolism, Endocrinology, and Diabetology, Yamagata University Faculty of Medicine, 2-2-2 Iida-nishi, Yamagata 990-9585, Japan; Tel: +81-23-628-5316; Fax: +81-23-628-5318;
E-mail: arawaka@med.id.yamagata-u.ac.jp

PATHOLOGICAL INCLUSIONS AND MISFOLDED PROTEINS IN NEURODEGENERATIVE DISEASES

The most characteristic feature of many neurodegenerative diseases caused by protein misfolding is the occurrence of extra- or intracellular fibrillar structures of protein aggregates, which are observed microscopically as amyloid deposits or inclusions. AD is a late-onset dementing disorder and the most common neurodegenerative disease [10, 13]. As shown in Fig. (**1A**, **B**), two kinds of protein aggregates are observed in AD: senile plaques and neurofibrillary tangles. Senile plaques are extracellular amyloid deposits composed of amyloid beta (Abeta), a 39–43-amino acid proteolytic fragment of amyloid precursor protein (APP) [10, 13]. Neurofibrillary tangles are another pathological hallmark of AD [10, 13]. They are intracytoplasmic inclusions composed of microtubule-associated protein tau [10, 13]. Which abnormal structures are formed at an earlier stage of the pathogenic mechanism has been discussed. However, in familial forms of AD, genetic studies provide a strong clue for this issue. Inherited mutations in genes encoding APP or presenilins, which cleave APP to release Abeta, cause familial AD. In contrast, inherited mutations in tau cause a less common dementing disorder, frontotemporal dementia with parkinsonism linked to chromosome 17 (FTDP-17). FTDP-17 patients have neurofibrillary tangles containing tau without extensive deposition of Abeta [10, 13]. PD is a representative movement disorder and the second most common neurode-

1389-2010/10 $55.00+.00

generative disease after AD [13-16]. PD is characterized clinically by resting tremor, rigidity, bradykinesia and postural instability. Pathologically, it is characterized by the presence of intracytoplasmic inclusions, called Lewy bodies, in the surviving dopaminergic neurons, as shown in Fig. (**1C**) [13-17]. The major component of Lewy bodies is alpha-synuclein [14, 15, 17]. Alpha-synuclein is also identified as a gene responsible for rare familial forms of PD [13]. ALS is relatively rare, but it is a fatal neurodegenerative disease in which motor neurons of the spinal cord and brain stem die, resulting in progressive paralysis and respiratory failure [13, 18]. A small fraction of ALS occurs as a familial form; SOD1 is one of the causative genes of familial ALS [18, 19]. Intracytoplasmic inclusions containing misfolded SOD1 are found in motor neurons of familial ALS patients with *SOD1* mutations [13]. HD is an autosomal dominant, inherited disease [20]. HD is caused by the expansion of CAG nucleotide repeats in the *huntingtin* gene [21], and the mutant gene product, polyglutamine-expanded huntingtin, forms intranuclear inclusions [10, 13]. The toxic role of fibrillar aggregates of disease-associated proteins in the pathogenesis remains unclear, and the question whether fibrils are a cause of neurodegeneration or a by-product of the neuronal protective machinery is still unanswered. Recent work on prefibrillar intermediates, defined in this review as all intermediates before conversion into mature fibrils, has provided an important insight into how toxic proteins lead to neuronal dysfunction and degeneration.

PREFIBRILLAR INTERMEDIATES IN FIBRIL FORMATION

In general, the main polypeptide chain and the hydrophobic side chains of globular proteins are largely buried within a folded structure. When they are exposed by partly unfolding or misfolding, the protein can become aggregated. Aggregation of proteins to the beta-sheet-rich fibril structure is a complex process, but it seems to undergo similar steps as in the following model (Fig. **2**) [7, 22-24]. The first step is the conversion of monomeric proteins from the native conformation to the misfolded conformation, and then oligomeric intermediates are formed. These early prefibrillar aggregates then change into protofibrils [25-27]. Protofibrils are observed by electron microscopy (EM) or atomic force microscopy (AFM) as short, thin, sometimes curly, fibrillar species [22, 25-27]. Some of these structures eventually assemble into mature fibrils by hydrophobic interaction and beta-sheet formation. There also exists a different pathway that diverts misfolded species or protofibrils from the formation of fibrils to the formation of amorphous aggregates [23].

Accumulating lines of evidence show that soluble oligomers are toxic intermediates leading to neuronal dysfunction and degeneration. They are detectable in mammalian cultured cells, the transgenic mice brains and human brains [8, 28-30]. This raises the question as to what corresponds to soluble oligomers in the above model of fibril formation. This may be difficult to answer, because soluble oligomers and protofibrils are defined using different methodologies. Soluble oligomers are assemblies that cannot be pelleted from physiological solutions by high-speed centrifugation [29, 30]. On the other hand, protofibrils are defined by their morphology under EM or AFM [29, 30]. All the morphologically identifiable intermediates seem unlikely to fulfill the definition of soluble oligomers completely [11, 30]. In addition, it should be noted that most of morphologically identifiable intermediates are only observed in *in vitro* fibrillization assays of synthetic peptides or purified recombinant proteins [29, 30]. Maeda, *et al.* reported to find granular tau oligomers in human AD brains by using AFM [31]. They detected granular tau oligomers from soluble fractions of AD brain extracts [31]. While it is unclear whether granular tau oligomers are recovered exclusively in the soluble fractions and whether granular oligomers truly convert to mature fibrils, this study may present a link between morphologically identifiable intermediates and soluble oligomers.

PREFIBRILLAR INTERMEDIATES AS TOXIC SPECIES IN FIBRIL FORMATION

In the pathogenesis of AD, the toxic properties of fibrillar aggregates have long been debated [32]. For example, the finding that the number of senile plaques in the brain does not correlate well with the degree of cognitive impairment is unexplained by the toxicity of fibrils [33]. On the other hand, soluble Abeta peptide concentration has been reported to

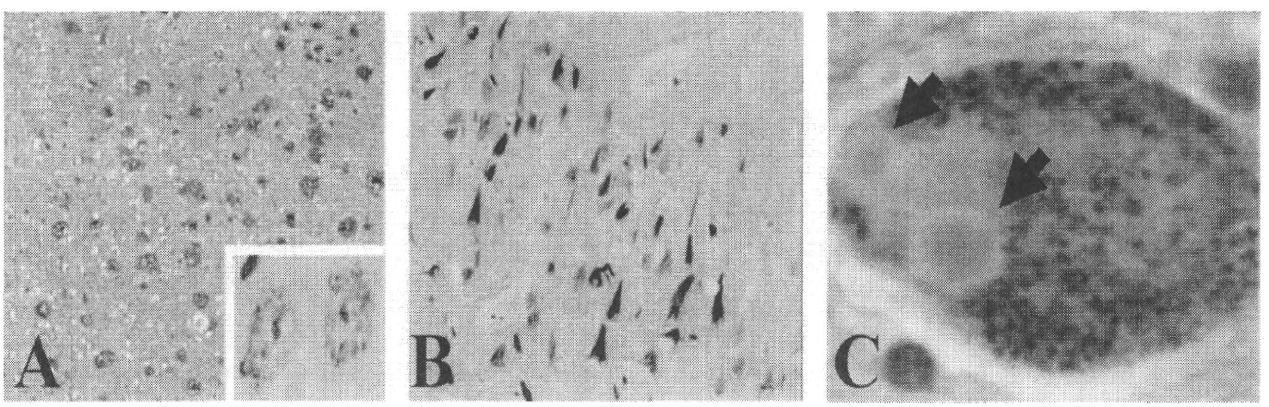

Fig. (1). Neuropathological deposits and inclusions as characteristic hallmarks of Alzheimer's disease (AD) and Parkinson's disease (PD). **(A)** Silver staining shows that extracellular deposits of senile plaques in the cerebral cortex of AD. Senile plaques are immunopositive for Abeta (inset). **(B)** Silver staining shows intracytoplasmic inclusions, neurofibrillary tangles, in the cerebral cortex of AD. **(C)** H&E staining shows a dopaminergic neuron in substantia nigra contains Lewy bodies (indicated by arrows) with surrounding halos.

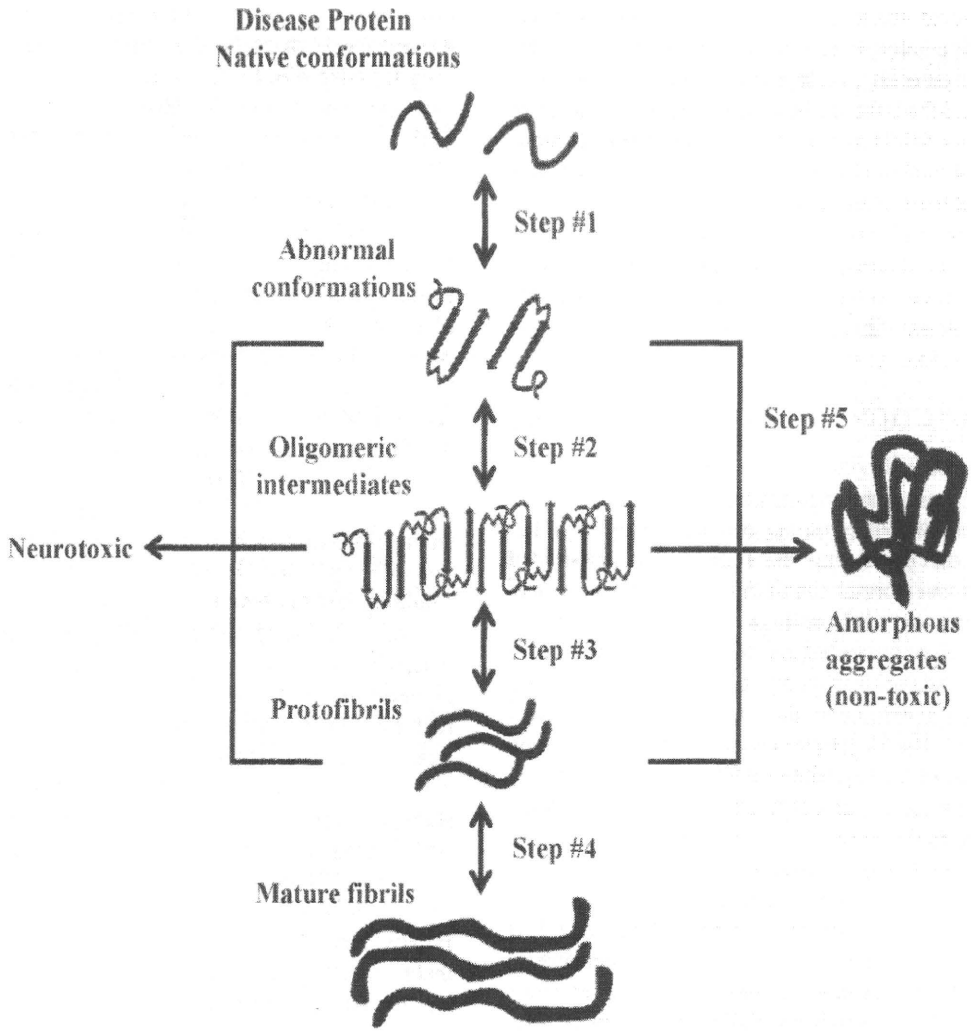

Fig. (2). A model of fibril formation of misfolded proteins. There are five possible junctures where heat shock proteins (HSPs) could act. HSPs may modulate the conversion between native conformations and abnormal conformations (step #1), between abnormal conformations and oligomeric species (step #2), between oligomeric species and protofibrils (step #3), between protofibrils and mature fibrils (step #4) and between each of prefibrillar aggregates and amorphous aggregates (step #5).

correlate better with synaptic loss and the density of neurofibrillary tangles than insoluble Abeta [34, 35], suggesting that soluble Abeta oligomers may represent the main toxic species. Walsh, *et al.* demonstrated that cerebral microinjection of cultured conditioned medium containing soluble oligomers (non-synthetic, naturally secreted soluble oligomers) and abundant monomers (but no amyloid fibrils) potently inhibited hippocampal long-term potentiation (LTP) in adult rats [28]. Pretreatment of the medium with a protease that selectively degrades Abeta monomers but not oligomers failed to prevent LTP inhibition [28]. Also, naturally secreted soluble oligomers can impair the memory of a complex learned behavior in rats [36], and decrease dendritic spine density in hippocampal slice cultures [37]. These findings have supported the soluble oligomer hypothesis. Recently, Tomiyama, *et al.* reported direct evidence for this hypothesis by discovering a novel APP mutation [the deletion of codon 693 (E693Δ), which produces Abeta lacking glutamate at position 22 (E22Δ)] in a Japanese pedigree with Alzheimer's-type dementia [38]. E22Δ Abeta showed the unique property of enhanced oligomerization but not fibrillization *in vitro*, and microinjection of synthetic E22Δ Abeta peptide inhibited hippocampal LTP in rats [38]. These findings suggest that the E693Δ mutation in APP causes synaptic impairment leading to Alzheimer's-type dementia by generation of Abeta oligomers. Also, Maeda, *et al.* reported that granular tau oligomers are detected in an early stage (Braak-stage I) of AD brains [31]. They suggested that increases in granular tau oligomer levels represent an early sign of neurofibrillary tangles formation in AD [31]. However, it remains unclear whether granular tau oligomers are toxic species in tau aggregation. In studies on PD, oxidation-induced dopamine adducts inhibit alpha-synuclein fibril formation, but cause accumulation of alpha-synuclein protofibrils [39]. In addition, alpha-synuclein protofibrils pre-formed *in vitro* have been reported to transiently permeabilize vesicular membranes, predisposing cultured cells to apoptosis [40-42]. Consistent with the toxic role of prefibrillar intermediates in AD and PD, disruption of microtubules with nocodazole in a yeast model of huntingtin aggregation revealed a glutamine length-dependent toxicity under conditions where the huntingtin protein existed in a nonfibrillar state [43]. These experiments indicate that prefibrillar intermediates, including soluble oligomers and protofibrils, play a toxic role in fibril

formation. However, the toxicity of prefibrillar intermediates remains to be elucidated, because whether soluble oligomers are identical to, or even overlap with, protofibrils is undetermined, as described above. In addition, whether the toxic species of mutant SOD1 are misfolded monomeric proteins or prefibrillar intermediates is unclear. Although copper-induced oxidation of metal-depleted SOD1 is reported to cause aggregation into pore-like structures, the toxicity of pore-like SOD1 is unknown [44]. Furthermore, the toxic role of fibrils seems to be exclusive, because senile plaques containing mature Abeta fibrils always accompany with dystrophic neurites [29].

GENERAL FUNCTION OF HSPS IN FIBRIL FORMATION

HSPs contribute to the maintenance of intracellular homeostasis by assisting the folding of many newly synthesized proteins and preventing the formation of misfolded proteins, both under normal conditions including aging, and a variety of stresses, such as high temperature, hypoxia, ischemia and glucose deprivation [45, 46]. HSPs form a large family of evolutionarily conserved proteins and are usually classified according to their molecular weight, such as Hsp40, Hsp60, Hsp70, Hsp90, Hsp100 and the so-called small Hsp proteins [45, 46]. The protective effect of HSPs is attributed to their molecular chaperone function, facilitating nascent protein folding, refolding or degradation of misfolded proteins. Hsp70 and chaperonin proteins (Hsp60 proteins) recognize the hydrophobic amino acid side-chains that are exposed in misfolded proteins and promote their folding in an ATP-dependent manner [45]. Hsp70 prevents protein aggregation by folding intramolecularly misfolded segments and by shielding the interactive surfaces of misfolded polypeptides [45]. Hsp70 cooperates in this function with Hsp40 proteins [45]. Interaction of substrates with Hsp70 is mediated by the so-called J domain, which is present in all Hsp40 proteins [46]. Hsp40 proteins also interact directly with unfolded polypeptides and can recruit Hsp70 to protein substrates [46]. In addition, the J-domain of Hsp40 activates the Hsp70 ATPase, catalyzing the formation of ADP-bound Hsp70, which binds protein substrate tightly [23]. Hsp70 also cooperates in this function with a nucleotide-exchange factor, Bag-1, in the eukaryotic cytosol [47, 48]. Another chaperone protein, Hsp104, has a remarkable ability to resolubilize protein aggregates and return proteins to their normal enzymatic activities in cooperation with Hsp70 and Hsp40 [49-51]. Hsp104 is expressed in fungi, plants and bacteria, but it has been lost from metazoan lineages [51]. The eukaryotic chaperonin, TRiC/CCT, receives misfolded proteins from Hsp70 and alters their aggregation state from fibril formation to non-toxic oligomers and amorphous aggregates [46, 52-54].

HSP-TARGETED INTERMEDIATES IN FIBRIL FORMATION

Which intermediates do HSPs recognize? In the model of fibril formation (Fig. **2**), there are five possible junctures where HSPs could act. HSPs could modulate the conversion between native conformations and abnormal conformations (step #1), between abnormal conformations and oligomeric species (step #2), between oligomeric species and protofibrils (step #3), between protofibrils and mature fibrils (step #4) and between prefibrillar aggregates and amorphous aggregates (step #5). *In vitro* studies on Abeta have shown that the combination of Hsp70, Hsp40 and Hsp90 inhibited Abeta fibril formation [55]. When the mixture of Hsp70, Hsp40 and Hsp90 was co-incubated with preformed mature fibrils, there was little change in the fibrils. However, when the mixture was added to preformed soluble oligomers, the soluble oligomers changed structure to become less defined and more diffuse. In this study, the authors presented EM analysis of oligomers; however, there was no discussion regarding whether these oligomers were the same as protofibrils or other intermediates [55]. Also, Dou, *et al.* examined the effect of Hsp70 and Hsp90 on tau aggregation by treating cultured cells with geldanamycin [56]. Geladamycin is a chemical compound that disrupts interaction between Hsp90 and heat-shock factor (HSF) 1 triggering a heat shock response, leading to increases in Hsp70 and Hsp90 expressions. Induction of Hsp70 and Hsp90 by geldanamycin increased tau solubility and tau binding to microtubules, resulted in reduction of insoluble tau levels [56]. In this study, it is unclear whether soluble tau represents species in the normal pool; however, treatment with geldanamycin reduced tau aggregation trapped by nitrocellulose filter. This finding suggests that induction of Hsp70 and Hsp90 may suppress tau aggregation before step #4 in Fig. (**2**). In an *in vitro* fibrillization study of alpha-synuclein, Hsp70 inhibited alpha-synuclein fibril formation through interaction with prefibrillar alpha-synuclein [57]. Because the authors supposed that prefibrillar alpha-synuclein was protofibrils, the results suggested that Hsp70 prevented the conversion between protofibrils and mature fibrils (step #4 in Fig. **2**). In an *in vitro* study on mutant huntingtin with expanded polyglutamine repeats, Hsp70 and Hsp40 modulated the formation of polyglutamine aggregates by partitioning monomeric conformations and disfavoring the accretion of spherical and annular oligomers (steps #1, 2 or 3 in Fig. **2**) [58]. In cultured cells, overexpression of Hsp70 and Hsp40 diverted the polyglutamine aggregation pathway from the formation of fibrils to the formation of amorphous and SDS-soluble aggregates (step #5 in Fig. **2**) [59]. In cultured mammalian cells, we previously reported that overexpression of Hsp70 and Hsp40 decreased the formation of Triton X-100-insoluble/SDS-soluble oligomers of familial ALS-linked mutant SOD1, resulting in the attenuation of highly insoluble aggregates [60]. Hsp70 and Hsp40 also attenuated accumulation of Triton X-100-insoluble/SDS-soluble monomers [60]. These findings suggest that Hsp70 and Hsp40 prevent the conversion of mutant SOD1 protein at step #1 in Fig. (**2**). All the above studies show that Hsp70 and Hsp40 can suppress fibril formation; however, the earliest intermediates targeted by Hsp70 and Hsp40 are unknown. Although Hsp70 and Hsp40 may have the ability to recognize various prefibrillar intermediates, it is unknown whether Hsp70 and Hsp40 recognize intermediates of different disease-associated proteins in the same manner. There may be variability in the exposed hydrophobic regions of misfolded proteins and prefibrillar intermediates for each disease-associated protein, causing a difference in Hsp70 and Hsp40 substrate recognition. To understand HSP-mediated targeting of prefibrillar intermediates, it will be necessary to compare the formation of prefibrillar intermediates defined in the same way and with easily reproducible experiments.

THE AMELIORATIVE EFFECT OF HSPS IN ANIMAL MODELS OF NEURODEGENERATIVE DISEASES

As described above, *in vitro* studies have not yet revealed whether HSPs specifically target monomeric species with abnormal conformations, soluble oligomers or protofibrils. If HSPs prevent only the conversion from protofibrils to mature fibrils, it is possible that soluble oligomers and protofibrils could continue to impair neuronal function. We next discuss the ameliorative effect of HSPs on fibril formation in *in vivo* models of neurodegenerative diseases. In an alpha-synuclein transgenic fly model of PD, overexpression of Hsp70 suppressed the loss of dopaminergic neurons, while overexpression of dominant-negative mutant Hsp70 significantly promoted alpha-synuclein toxicity [61, 62]. Also, in a 1-methyl-4-phenyl-1,2,3,6-tetrahydropyridine (MPTP)-induced mouse model of PD, Shen, *et al.* reported that geldanamycin increased residual dopamine content and protected dopaminergic neurons from death [63]. They showed that the protective mechanism of geldanamycin was associated with an increase in Hsp70 and a reduction in cytosolic Hsp90. In a *C. elegans* model of tauopathy, overexoression of Hsp70 improved dysfunction of neurons overexpressing FTDP-17 linked mutant tau [64]. In fly models of polyglutamine expansion diseases, there are several reports showing the ameliorative effects of Hsp70 and Hsp40 [65-67]. These studies reveal that overexpression of Hsp70 and Hsp40 suppresses the degenerative phenotype. Also, in a mouse model of spinocerebellar ataxia 1, overexpression of Hsp70 reduced pathological changes and abnormal behavioral phenotypes [68].

Although *in vivo* models of PD and polyglutamine expansion diseases show the beneficial effect of overexpressed Hsp70 on neurodegeneration, the protective effect of Hsp70 is controversial in SOD1 transgenic mouse models of ALS [69, 70]. One may speculate a difference in the expression levels of overexpressed Hsp70 in each transgenic mouse line, and a requirement for co-overexpression of Hsp40 [1]. The latter possibility is supported by evidence that treatment with arimoclomol significantly rescues loss of motor neurons, resulting in improved muscle function and an increase in survival in mutant SOD1 transgenic mice [1, 2]. This finding suggests that co-induction of multiple HSPs may be more effective than single overexpression of Hsp70 [1]. Taken together, many studies indicate that an increase in HSP expression can ameliorate disease phenotypes. In the next section, we discuss the relationship between HSP-targeted intermediates and the therapeutic potential of HSPs in chronically progressive neurodegenerative diseases.

THERAPEUTIC POTENTIAL OF HSPS: LESSONS FROM ACCUMULATION OF MISFOLDED PROTEINS IN NEURODEGENERATIVE DISEASED BRAINS

One of the beneficial aspects of HSPs is that they can directly target toxic prefibrillar intermediates, including soluble oligomers and protofibrils, which occur in the early stages of fibril formation. This indicates that HSPs have a remarkable potential to resolve the essential pathological changes of neurodegenerative diseases. In normal human brains, accumulation of insoluble Abeta starts in the late 40s, and it increases exponentially during the next 20 years [71]. The Abeta accumulation reaches a plateau at about 70 years of age [71]. This finding suggests that insoluble Abeta in the brain has already considerably accumulated by the time that AD patients develop dementia (Fig. **3A**). This phenomenon may be similar in other diseases. To make HSP-based therapy effective, induction of HSPs should be started as soon as possible. The development of methods for early diagnosis (biological markers and imaging), to identify patients with neurodegenerative diseases before the onset of symptoms, is important for HSP-based therapy (Fig. **3A**).

Another beneficial aspect is that HSPs can recognize a broad range of misfolded proteins. This implies an ability to inhibit the accumulation of not only disease-associated prefibrillar intermediates but also unknown misfolded proteins, which might be secondarily generated as a result of disease progression. The phase I clinical trial of active immunization against $Abeta_{42}$ has provided suggestive findings for the pathogenesis of AD and other neurodegenerative diseases [72]. A six-year prospective follow-up of 80 AD patients in this trial reported that immunization against Abeta succeeded in removing brain amyloid plaques, but it failed to improve cognitive function and survival [72]. This result indicates that clearance of amyloid plaques alone does not prevent the progression of neurodegeneration. One possibility is that toxic soluble oligomers may remain. Also, the prior Abeta accumulation may have already initiated secondary cascades leading to neurodegeneration, such as accumulation of misfolded tau [73], as shown in Fig. (**3B**). Although other neurodegenerative diseases, such as PD and HD, primarily show only one characteristic inclusion type, this secondary cascade hypothesis might be expanded to include these diseases. If the initial accumulation of disease-associated protein could trigger misfolding of unknown proteins as a secondary cascade, the newly misfolded proteins might exert the toxic effect by the formation of prefibrillar intermediates (Fig. **3B**). At the present time this possibility cannot be excluded, because misfolded proteins, even those hitherto not associated with disease, can exert toxicity [74]. The ability of HSPs to target soluble oligomers, and their low substrate specificity, confer strong advantages to HSPs in resolving this difficult problem (Fig. **3C**) [75]. Another implication is that fly and mouse models may have limited usefulness in assessing therapeutic efficacy for chronic neurodegenerative diseases, because the protective effect of immunization with Abeta on neuronal degeneration was supported by many studies using *in vivo* mouse models [76, 77]. One significant difference however, is that the disease progression period in human brains is so much longer than that in fly and mouse models. This time difference might provide the opportunity for accumulation of different misfolded proteins as a secondary cascade in human diseased brains.

CONCLUSIONS AND PERSPECTIVES

Recent studies on the pathogenesis of neurodegenerative diseases have provided data supporting the soluble oligomer hypothesis, *i.e.*, that soluble oligomers play the toxic role in synaptic dysfunction and neurodegeneration [8, 29, 30, 78]. This trend increases the therapeutic potential of HSPs, when compared with treatments targeting a single misfolded pro-

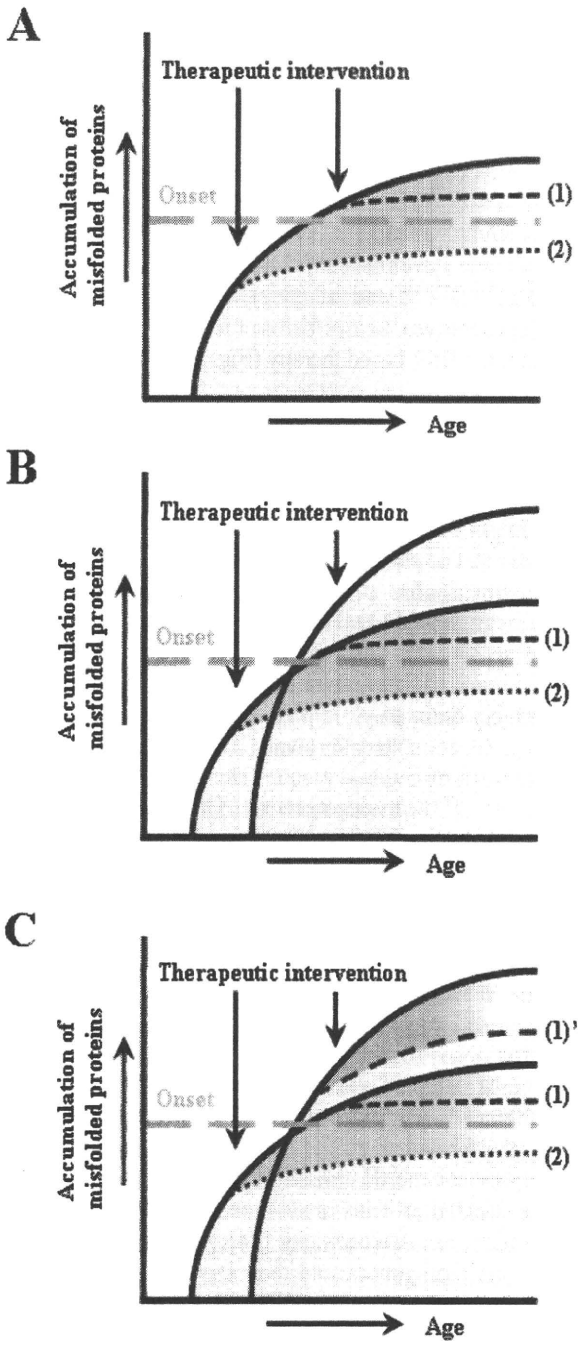

Fig. (3). Protein misfolding cascade hypothesis in neurodegenerative diseases and the beneficial aspect of HSP-based therapy. **(A)** In the case of single disease-associated protein misfolding. If the disease is caused by accumulation of a single misfolded protein, misfolded protein considerably accumulates before the onset of the disease symptoms. When started therapeutic intervention against the single molecule after the onset, it can suppress disease progression (1). When started therapeutic intervention against the single molecule before the onset, it can inhibit the onset (2). **(B)** In the case that first accumulation of misfolded protein leads to the second cascade of accumulation of different misfolded protein. If started therapeutic intervention against the single molecule after the onset, the therapy fails to suppress the second cascade and disease progression. **(C)** In the case similar to **(B)** with the therapeutic intervention by HSPs. HSPs have an ability to attenuate a broad range of misfolded proteins. If started therapeutic intervention by HSPs even after the onset, HSPs might be able to suppress the first and second cascades of accumulation of toxic misfolded proteins (1 and 1').

tein, because uniquely, HSPs can prevent accumulation of prefibrillar intermediates of multiple proteins [75]. This hypothesis has been constructed and tested largely using *in vitro* and *in vivo* studies on AD and polyglutamine expansion diseases [10, 29, 30]. In the case of PD, soluble oligomers of alpha-synuclein can be induced by adding polyunsaturated fatty acids to cultured cells [79-81], and fatty acid-associated soluble oligomers of alpha-synuclein are observed in alpha-synuclein transgenic mice brains and PD brains [79]. However, to detect fatty acid-associated soluble oligomers of alpha-synuclein, it is necessary to treat cell lysates and brain homogenates with a lipid removal procedure, such as heat or methanol/chloroform [79-81]. Naturally generated soluble oligomers of alpha-synuclein in cultured cells and brains are not found in a readily reproducible way, making it difficult to assess the toxic role of soluble alpha-synuclein oligomers in the pathogenesis of PD. In ALS, testing the hypothesis on mutant SOD1 is not enough. In a previous report, we found that Triton X-100 insoluble/SDS-soluble SOD1 monomers and dimers were significantly elevated before the onset of motor dysfunction in mutant SOD1 transgenic mice, while alteration of SOD1 solubility was not detected in wild-type SOD1 transgenic mice [60]. The expression of Hsp70 and Hsp40 was increased in parallel in Triton X-100-insoluble/SDS-soluble fractions before the onset of motor dysfunction [60]. Our data suggest that Triton X-100-insoluble/SDS-soluble mutant SOD1 appears as early, misfolded intermediates when their concentration exceeds the capacity of HSPs to remove them. Wang, *et al.* reported that mutant SOD1 monomers progressively alter in their phosphate-buffered saline (PBS)-insoluble/SDS-soluble properties with aging in mutant SOD1 transgenic mice [82]. They also found that PBS-soluble mutant SOD1 captured heat shock cognate protein 70 (Hsc70) [82]. These data suggest that SDS-soluble species of mutant SOD1 are associated with the early stages of the disease, and HSPs play a role in the mutant SOD1 fibril formation. It is important to collect further experimental data on the toxic role of soluble oligomers of mutant SOD1. Recently, mutations in TAR DNA binding protein (TARDBP/TDP-43) were identified to cause a subgroup of familial ALS. Studies on the TDP-43 protein may provide an insight into the pathogenesis of ALS [83-88]. In some cases, clinical trials in neurodegenerative diseases seem likely to start before sufficient evidence in favor of specific drugs or treatments has been accumulated. Even for arimoclomol, as Kalmar and Greensmith clearly pointed out, there are some significant hurdles that must be overcome before HSP-based treatment can be successful [89]. The drug needs to ensure that the induction of HSPs occurs at the right place (*i.e.*, cell specificity), at the right time in the disease progression and that all co-chaperones are present at the proper levels [89].

In this review, we especially discuss the refolding function of HSPs against accumulation of toxic misfolded proteins in neurodegenerative diseases. However, HSPs exert various functions to maintain intracellular environment [45, 46]. HSPs mediate translocation of proteins across cellular membranes and they facilitate the transfer of misfolded proteins to the proteasome [45, 46] or lysosome [90] for degradation. For example, in mutant tau transgenic mice, treatment with Hsp90 inhibitor, EC102, is reported to reduce the

expression levels of phosphorylated tau, which seems to play a main toxic role in tauopathies [91]. In this case, a proposed mechanism of EC102 is complex. When presented abnormally phophorylayed tau, Hsp70, Hsp40 and Hsp90 first act to refold phosphorylated tau and return to its normal pool. However, when refolding is subverted by Hsp90 inhibition, phosphorylated tau is polyubiqutinated by carboxyl terminus of Hsp70-interacting protein (CHIP) and targeted to the proteasome degradation pathway [91, 92]. This shows a novel way to manipulate the HSP system by chemicals other than simply facilitating the refolding of prefibrillar intermediates by induction of HSPs. In addition to these functions, HSPs affect signal transduction cascades that mediate transcriptional responses to stress for the suppression of apoptosis [45, 46, 93]. Furthermore, HSPs is discussed as extracellular signals for receptor-mediated signaling of inflammation in neurodegenerative diseases [94, 95]. Thus, we need to see the protective effects of HSPs on neurodegeneration from a variety of HSP functions. To avoid misjudgment of the therapeutic potential of HSPs, it is crucial to assess repeatedly the appropriateness of the background concept by both *in vitro* and *in vivo* experiments for each neurodegenerative disease.

ABBREVIATIONS

HSP	=	Heat shock protein
AD	=	Alzheimer's disease
FTDP-17	=	Frontotemporal dementia with parkinsonism linked to chromosome 17
PD	=	Parkinson's disease
ALS	=	Amyotrophic lateral sclerosis
HD	=	Huntington's disease
SOD1	=	Cu/Zn superoxide dismutase
Abeta	=	Amyloid beta
APP	=	Amyloid precursor protein
EM	=	Electron microscopy
AFM	=	Atomic force microscopy
HSF	=	Heat-shock factor
Hsc70	=	Heat shock cognate protein 70
MPTP	=	1-methyl-4-phenyl-1,2,3,6-tetrahydropyridine
TARDBP	=	TAR DNA binding protein
CHIP	=	Carboxyl terminus of Hsp70-interacting protein

ACKNOWLEDGEMENTS

This work was supported in part by a Grant-in-Aid from the Global COE Program (F03) of the Japan Society for the Promotion of Science (T.K.).

REFERENCES

[1] Kieran, D.; Kalmar, B.; Dick, J.R.; Riddoch-Contreras, J.; Burnstock, G.; Greensmith, L. Treatment with arimoclomol, a coinducer of heat shock proteins, delays disease progression in ALS mice. *Nat. Med.*, **2004**, *10*(4), 402-405.

[2] Kalmar, B.; Novoselov, S.; Gray, A.; Cheetham, M.E.; Margulis, B.; Greensmith, L. Late stage treatment with arimoclomol delays disease progression and prevents protein aggregation in the SOD1 mouse model of ALS. *J. Neurochem.*, **2008**, *107*(2), 339-350.

[3] Cudkowicz, M.E.; Shefner, J.M.; Simpson, E.; Grasso, D.; Yu, H.; Zhang, H.; Shui, A.; Schoenfeld, D.; Brown, R.H.; Wieland, S.; Barber, J.R. Arimoclomol at dosages up to 300 mg/day is well tolerated and safe in amyotrophic lateral sclerosis. *Muscle Nerve*, **2008**, *38*(1), 837-844.

[4] Balch, W.E.; Morimoto, R.I.; Dillin, A.; Kelly, J.W. Adapting proteostasis for disease intervention. *Science*, **2008**, *319*(5865), 916-919.

[5] Taylor, J.P.; Hardy, J.; Fischbeck, K.H. Toxic proteins in neurodegenerative disease. *Science*, **2002**, *296*(5575), 1991-1995.

[6] Bates, G. Huntingtin aggregation and toxicity in Huntington's disease. *Lancet*, **2003**, *361*(9369), 1642-1644.

[7] Caughey, B.; Lansbury, P.T. Protofibrils, pores, fibrils, and neurodegeneration: separating the responsible protein aggregates from the innocent bystanders. *Annu. Rev. Neurosci.*, **2003**, *26*, 267-298.

[8] Kayed, R.; Head, E.; Thompson, J.L.; McIntire, T.M.; Milton, S.C.; Cotman, C.W.; Glabe, C.G. Common structure of soluble amyloid oligomers implies common mechanism of pathogenesis. *Science*, **2003**, *300*(5618), 486-489.

[9] Nussbaum, R.L.; Ellis, C.E. Alzheimer's disease and Parkinson's disease. *N. Engl. J. Med.*, **2003**, *348*(14), 1356-1364.

[10] Selkoe, D.J. Folding proteins in fatal ways. *Nature*, **2003**, *426*(6968), 900-904.

[11] Muchowski, P.J.; Wacker, J.L. Modulation of neurodegeneration by molecular chaperones. *Nat. Rev. Neurosci.*, **2005**, *6*(1), 11-22.

[12] Hutt, D.M.; Powers, E.T.; Balch, W.E. The proteostasis boundary in misfolding diseases of membrane traffic. *FEBS Lett.*, **2009**, *583*(16), 2639-2646.

[13] Ross, C.A.; Poirier, M.A. Protein aggregation and neurodegenerative disease. *Nat. Med.*, **2004**, *10* (Suppl.), S10-17.

[14] Dawson, T.M.; Dawson, V.L. Molecular pathways of neurodegeneration in Parkinson's disease. *Science*, **2003**, *302*(5646), 819-822.

[15] Eriksen, J.L.; Dawson, T.M.; Dickson, D.W.; Petrucelli, L. Caught in the act: alpha-synuclein is the culprit in Parkinson's disease. *Neuron*, **2003**, *40*(3), 453-456.

[16] Lee, V.M.; Trojanowski, J.Q. Mechanisms of Parkinson's disease linked to pathological alpha-synuclein: new targets for drug discovery. *Neuron*, **2006**, *52*(1), 33-38.

[17] Spillantini, M.G.; Schmidt, M.L.; Lee, V.M.; Trojanowski, J.Q.; Jakes, R.; Goedert, M. Alpha-synuclein in Lewy bodies. *Nature*, **1997**, *388*(6645), 839-840.

[18] Cudkowicz, M.E.; McKenna-Yasek, D.; Sapp, P.E.; Chin, W.; Geller, B.; Hayden, D.L.; Schoenfeld, D.A.; Hosler, B.A.; Horvitz, H.R.; Brown, R.H. Epidemiology of mutations in superoxide dismutase in amyotrophic lateral sclerosis. *Ann. Neurol.*, **1997**, *41*(2), 210-221.

[19] Rosen, D.R.; Siddique, T.; Patterson, D.; Figlewicz, D.A.; Sapp, P.; Hentati, A.; Donaldson, D.; Goto, J.; O'Regan, J.P.; Deng, H.X.; Rahmani, Z.; Krizus, A.; McKenna-Yasek, D.; Cayabyab, A.; Gaston, S.M.; Berger, R.; Tanzi, R.E.; Halperin, J.J.; Herzfeldt, B.; Van den Bergh, R.; Hung, W.; Bird, T.; Deng, G.; Mulder, D.W.; Smyth, C.; Laing, N.G.; Soriano, E.; Pericak-Vance, M.A.; Haines, J.; Rouleau, G.A.; Gusella, G.A.; Horvitz, H.R.; Brown, R.H. Mutations in Cu/Zn superoxide dismutase gene are associated with familial amyotrophic lateral sclerosis. *Nature*, **1993**, *362*(6415), 59-62.

[20] Zoghbi, H.Y.; Orr, H.T. Glutamine repeats and neurodegeneration. *Annu. Rev. Neurosci.*, **2000**, *23*, 217-247.

[21] MacDonald, M.E.; Ambrose, C.M.; Duyao, M.P.; Myers, R.H.; Lin, C.; Srinidhi, L.; Barnes, G.; Taylor, S.A.; James, M.; Groot, N.; MacFarlane, H.; Jenkins, B.; Anderson, M.A.; Wexler, N.S.; Gusella, J.F.; Bates, G.P.; Baxendale, S.; Hummerich, H.; Kirby, S.; North, M.; Youngman, S.; Mott, R.; Zehetner, G.; Sedlacek, Z.; Poustka, A.; Frischauf, A.; Lehrach, H.; Buckler, A.J.; Church, D.; Doucette-Stamm, L.; O'Donovan, M.C.; Riba-Ramirez, L.; Shah, M.; Stanton, V.P.; Strobel, S.A.; Draths, K.M.; Wales, J.L.; Dervan, P.; Housman, D.E.; Altherr, M.; Shiang, R.; Thompson, L.; Fielder, T.; Wasmuth, J.J.; Tagle, D.; Valdes, J.; Elmer, L.; Allard, M.; Castilla, L.; Swaroop, M.; Blanchard, K.; Collins and Russell Snell, F.S.; Holloway, T.; Gillespie, K.; Datson, N.; Harper, D.S.S. A novel gene containing a trinucleotide repeat that is expanded and

unstable on Huntington's disease chromosomes. *Cell*, **1993**, *72*(6), 971-983.

[22] Muchowski, P.J. Protein misfolding, amyloid formation, and neurodegeneration: a critical role for molecular chaperones? *Neuron*, **2002**, *35*(1), 9-12.

[23] Sakahira, H.; Breuer, P.; Hayer-Hartl, M.K.; Hartl, F.U. Molecular chaperones as modulators of polyglutamine protein aggregation and toxicity. *Proc. Natl. Acad. Sci. USA*, **2002**, *99* (Suppl. 4), 16412-16418.

[24] Dobson, C.M. Protein folding and misfolding. *Nature*, **2003**, *426*(6968), 884-890.

[25] Harper, J.D.; Wong, S.S.; Lieber, C.M.; Lansbury, P.T. Observation of metastable Abeta amyloid protofibrils by atomic force microscopy. *Chem. Biol.*, **1997**, *4*(2), 119-125.

[26] Hartley, D.M.; Walsh, D.M.; Ye, C.P.; Diehl, T.; Vasquez, S.; Vassilev, P.M.; Teplow, D.B.; Selkoe, D.J. Protofibrillar intermediates of amyloid beta-protein induce acute electrophysiological changes and progressive neurotoxicity in cortical neurons. *J. Neurosci.*, **1999**, *19*(20), 8876-8884.

[27] Walsh, D.M.; Hartley, D.M.; Kusumoto, Y.; Fezoui, Y.; Condron, M.M.; Lomakin, A.; Benedek, G.B.; Selkoe, D.J.; Teplow, D.B. Amyloid beta-protein fibrillogenesis. Structure and biological activity of protofibrillar intermediates. *J. Biol. Chem.*, **1999**, *274*(36), 25945-25952.

[28] Walsh, D.M.; Klyubin, I.; Fadeeva, J.V.; Cullen, W.K.; Anwyl, R.; Wolfe, M.S.; Rowan, M.J.; Selkoe, D.J. Naturally secreted oligomers of amyloid beta protein potently inhibit hippocampal long-term potentiation *in vivo*. *Nature*, **2002**, *416*(6880), 535-539.

[29] Haass, C.; Selkoe, D.J. Soluble protein oligomers in neurodegeneration: lessons from the Alzheimer's amyloid beta-peptide. *Nat. Rev. Mol. Cell Biol.*, **2007**, *8*(2), 101-112.

[30] Selkoe, D.J. Soluble oligomers of the amyloid beta-protein impair synaptic plasticity and behavior. *Behav. Brain Res.*, **2008**, *192*(1), 106-113.

[31] Maeda, S.; Sahara, N.; Saito, Y.; Murayama, S.; Ikai, A.; Takashima, A. Increased levels of granular tau oligomers: an early sign of brain aging and Alzheimer's disease. *Neurosci. Res.*, **2006**, *54*(3), 197-201.

[32] Lansbury, P.T.; Lashuel, H.A. A century-old debate on protein aggregation and neurodegeneration enters the clinic. *Nature*, **2006**, *443*(7113), 774-779.

[33] Hardy, J.; Selkoe, D.J. The amyloid hypothesis of Alzheimer's disease: progress and problems on the road to therapeutics. *Science*, **2002**, *297*(5580), 353-356.

[34] McLean, C.A.; Cherny, R.A.; Fraser, F.W.; Fuller, S.J.; Smith, M.J.; Beyreuther, K.; Bush, A.I.; Masters, C.L. Soluble pool of Abeta amyloid as a determinant of severity of neurodegeneration in Alzheimer's disease. *Ann. Neurol.*, **1999**, *46*(6), 860-866.

[35] Lue, L.F.; Kuo, Y.M.; Roher, A.E.; Brachova, L.; Shen, Y.; Sue, L.; Beach, T.; Kurth, J.H.; Rydel, R.E.; Rogers, J. Soluble amyloid beta peptide concentration as a predictor of synaptic change in Alzheimer's disease. *Am. J. Pathol.*, **1999**, *155*(3), 853-862.

[36] Cleary, J.P.; Walsh, D.M.; Hofmeister, J.J.; Shankar, G.M.; Kuskowski, M.A.; Selkoe, D.J.; Ashe, K.H. Natural oligomers of the amyloid-beta protein specifically disrupt cognitive function. *Nat. Neurosci.*, **2005**, *8*(1), 79-84.

[37] Shankar, G.M.; Bloodgood, B.L.; Townsend, M.; Walsh, D.M.; Selkoe, D.J.; Sabatini, B.L. Natural oligomers of the Alzheimer amyloid-beta protein induce reversible synapse loss by modulating an NMDA-type glutamate receptor-dependent signaling pathway. *J. Neurosci.*, **2007**, *27*(11), 2866-2875.

[38] Tomiyama, T.; Nagata, T.; Shimada, H.; Teraoka, R.; Fukushima, A.; Kanemitsu, H.; Takuma, H.; Kuwano, R.; Imagawa, M.; Ataka, S.; Wada, Y.; Yoshioka, E.; Nishizaki, T.; Watanabe, Y.; Mori, H. A new amyloid beta variant favoring oligomerization in Alzheimer's-type dementia. *Ann. Neurol.*, **2008**, *63*(3), 377-387.

[39] Conway, K.A.; Rochet, J.C.; Bieganski, R.M.; Lansbury, P.T., Jr. Kinetic stabilization of the alpha-synuclein protofibril by a dopamine-alpha-synuclein adduct. *Science*, **2001**, *294*(5545), 1346-1349.

[40] Volles, M.J.; Lee, S.J.; Rochet, J.C.; Shtilerman, M.D.; Ding, T.T.; Kessler, J.C.; Lansbury, P.T., Jr. Vesicle permeabilization by protofibrillar alpha-synuclein: implications for the pathogenesis and treatment of Parkinson's disease. *Biochemistry*, **2001**, *40*(26), 7812-7819.

[41] Volles, M.J.; Lansbury, P.T., Jr. Vesicle permeabilization by protofibrillar alpha-synuclein is sensitive to Parkinson's disease-linked mutations and occurs by a pore-like mechanism. *Biochemistry*, **2002**, *41*(14), 4595-4602.

[42] Volles, M.J.; Lansbury, P.T., Jr. Zeroing in on the pathogenic form of alpha-synuclein and its mechanism of neurotoxicity in Parkinson's disease. *Biochemistry*, **2003**, *42*(26), 7871-7878.

[43] Muchowski, P.J.; Ning, K.; D'Souza-Schorey, C.; Fields, S. Requirement of an intact microtubule cytoskeleton for aggregation and inclusion body formation by a mutant huntingtin fragment. *Proc. Natl. Acad. Sci. USA*, **2002**, *99*(2), 727-732.

[44] Chung, J.; Yang, H.; de Beus, M.D.; Ryu, C.Y.; Cho, K.; Colon, W. Cu/Zn superoxide dismutase can form pore-like structures. *Biochem. Biophys. Res. Commun.*, **2003**, *312*(4), 873-876.

[45] Hartl, F.U. Molecular chaperones in cellular protein folding. *Nature*, **1996**, *381*(6583), 571-579.

[46] Hartl, F.U.; Hayer-Hartl, M. Converging concepts of protein folding *in vitro* and *in vivo*. *Nat. Struct. Mol. Biol.*, **2009**, *16*(6), 574-581.

[47] Hohfeld, J.; Jentsch, S. GrpE-like regulation of the hsc70 chaperone by the anti-apoptotic protein BAG-1. *EMBO J.*, **1997**, *16*(20), 6209-6216.

[48] Hartl, F.U.; Hayer-Hartl, M. Molecular chaperones in the cytosol: from nascent chain to folded protein. *Science*, **2002**, *295*(5561), 1852-1858.

[49] Parsell, D.; Kowal, A.S.; Singer, M.A.; Lindquist, S. Protein disaggregation mediated by heat-shock protein Hsp104. *Nature*, **1994**, *372*(6505), 475-478.

[50] Glover, J.R.; Lindquist, S. Hsp104, Hsp70, and Hsp40: a novel chaperone system that rescues previously aggregated proteins. *Cell*, **1998**, *94*(1), 73-82.

[51] Lo Bianco, C.; Shorter, J.; Regulier, E.; Lashuel, H.; Iwatsubo, T.; Lindquist, S.; Aebischer, P. Hsp104 antagonizes alpha-synuclein aggregation and reduces dopaminergic degeneration in a rat model of Parkinson disease. *J. Clin. Invest.*, **2008**, *118*(9), 3087-3097.

[52] Behrends, C.; Langer, C.A.; Boteva, R.; Bottcher, U.M.; Stemp, M.J.; Schaffar, G.; Rao, B.V.; Giese, A.; Kretzschmar, H.; Siegers, K.; Hartl, F.U. Chaperonin TRiC promotes the assembly of polyQ expansion proteins into nontoxic oligomers. *Mol. Cell*, **2006**, *23*(6), 887-897.

[53] Kitamura, A.; Kubota, H.; Pack, C.G.; Matsumoto, G.; Hirayama, S.; Takahashi, Y.; Kimura, H.; Kinjo, M.; Morimoto, R.I.; Nagata, K. Cytosolic chaperonin prevents polyglutamine toxicity with altering the aggregation state. *Nat. Cell Biol.*, **2006**, *8*(10), 1163-1170.

[54] Tam, S.; Geller, R.; Spiess, C.; Frydman, J. The chaperonin TRiC controls polyglutamine aggregation and toxicity through subunit-specific interactions. *Nat. Cell Biol.*, **2006**, *8*(10), 1155-1162.

[55] Evans, C.G.; Wisen, S.; Gestwicki, J.E. Heat shock proteins 70 and 90 inhibit early stages of amyloid beta-(1-42) aggregation *in vitro*. *J. Biol. Chem.*, **2006**, *281*(44), 33182-33191.

[56] Dou, F.; Netzer, W.J.; Tanemura, K.; Li, F.; Hartl, F.U.; Takashima, A.; Gouras, G.K.; Greengard, P.; Xu, H. Chaperones increase association of tau protein with microtubules. *Proc. Natl. Acad. Sci. USA*, **2003**, *100*(2), 721-726.

[57] Huang, C.; Cheng, H.; Hao, S.; Zhou, H.; Zhang, X.; Gao, J.; Sun, Q.H.; Hu, H.; Wang, C.C. Heat shock protein 70 inhibits alpha-synuclein fibril formation via interactions with diverse intermediates. *J. Mol. Biol.*, **2006**, *364*(3), 323-336.

[58] Wacker, J.L.; Zareie, M.H.; Fong, H.; Sarikaya, M.; Muchowski, P.J. Hsp70 and Hsp40 attenuate formation of spherical and annular polyglutamine oligomers by partitioning monomer. *Nat. Struct. Mol. Biol.*, **2004**, *11*(12), 1215-1222.

[59] Muchowski, P.J.; Schaffar, G.; Sittler, A.; Wanker, E.E.; Hayer-Hartl, M.K.; Hartl, F.U. Hsp70 and hsp40 chaperones can inhibit self-assembly of polyglutamine proteins into amyloid-like fibrils. *Proc. Natl. Acad. Sci. USA*, **2000**, *97*(14), 7841-7846.

[60] Koyama, S.; Arawaka, S.; Chang-Hong, R.; Wada, M.; Kawanami, T.; Kurita, K.; Kato, M.; Nagai, M.; Aoki, M.; Itoyama, Y.; Sobue, G.; Chan, P.H.; Kato, T. Alteration of familial ALS-linked mutant SOD1 solubility with disease progression: its modulation by the proteasome and Hsp70. *Biochem. Biophys. Res. Commun.*, **2006**, *343*(3), 719-730.

[61] Auluck, P.K.; Chan, H.Y.; Trojanowski, J.Q.; Lee, V.M.; Bonini, N.M. Chaperone suppression of alpha-synuclein toxicity in a Drosophila model for Parkinson's disease. *Science*, **2002**, *295*(5556), 865-868.

[62] Helfand, S.L. Neurobiology. Chaperones take flight. *Science*, **2002**, *295*(5556), 809-810.

[63] Shen, H.Y.; He, J.C.; Wang, Y.; Huang, Q.Y.; Chen, J.F. Geldanamycin induces heat shock protein 70 and protects against MPTP-induced dopaminergic neurotoxicity in mice. *J. Biol. Chem.*, **2005**, *280*(48), 39962-39969.

[64] Miyasaka, T.; Ding, Z.; Gengyo-Ando, K.; Oue, M.; Yamaguchi, H.; Mitani, S.; Ihara, Y. Progressive neurodegeneration in C. elegans model of tauopathy. *Neurobiol. Dis.*, **2005**, *20*(2), 372-383.

[65] Fernandez-Funez, P.; Nino-Rosales, M.L.; de Gouyon, B.; She, W.C.; Luchak, J.M.; Martinez, P.; Turiegano, E.; Benito, J.; Capovilla, M.; Skinner, P.J.; McCall, A.; Canal, I.; Orr, H.T.; Zoghbi, H.Y.; Botas, J. Identification of genes that modify ataxin-1-induced neurodegeneration. *Nature*, **2000**, *408*(6808), 101-106.

[66] Kazemi-Esfarjani, P.; Benzer, S. Genetic suppression of polyglutamine toxicity in Drosophila. *Science*, **2000**, *287*(5459), 1837-1840.

[67] Warrick, J.M.; Chan, H.Y.; Gray-Board, G.L.; Chai, Y.; Paulson, H.L.; Bonini, N.M. Suppression of polyglutamine-mediated neurodegeneration in Drosophila by the molecular chaperone HSP70. *Nat. Genet.*, **1999**, *23*(4), 425-428.

[68] Cummings, C.J.; Sun, Y.; Opal, P.; Antalffy, B.; Mestril, R.; Orr, H.T.; Dillmann, W.H.; Zoghbi, H.Y. Over-expression of inducible HSP70 chaperone suppresses neuropathology and improves motor function in SCA1 mice. *Hum. Mol. Genet.*, **2001**, *10*(14), 1511-1518.

[69] Liu, J.; Shinobu, L.A.; Ward, C.M.; Young, D.; Cleveland, D.W. Elevation of the Hsp70 chaperone does not effect toxicity in mouse models of familial amyotrophic lateral sclerosis. *J. Neurochem.*, **2005**, *93*(4), 875-882.

[70] Gifondorwa, D.J.; Robinson, M.B.; Hayes, C.D.; Taylor, A.R.; Prevette, D.M.; Oppenheim, R.W.; Caress, J.; Milligan, C.E. Exogenous delivery of heat shock protein 70 increases lifespan in a mouse model of amyotrophic lateral sclerosis. *J. Neurosci.*, **2007**, *27*(48), 13173-13180.

[71] Morishima-Kawashima, M.; Ihara, Y. Alzheimer's disease: beta-Amyloid protein and tau. *J. Neurosci. Res.*, **2002**, *70*(3), 392-401.

[72] Holmes, C.; Boche, D.; Wilkinson, D.; Yadegarfar, G.; Hopkins, V.; Bayer, A.; Jones, R.W.; Bullock, R.; Love, S.; Neal, J.W.; Zotova, E.; Nicoll, J.A. Long-term effects of Abeta42 immunisation in Alzheimer's disease: follow-up of a randomised, placebo-controlled phase I trial. *Lancet*, **2008**, *372*(9634), 216-223.

[73] St George-Hyslop, P.H.; Morris, J.C. Will anti-amyloid therapies work for Alzheimer's disease? *Lancet*, **2008**, *372*(9634), 180-182.

[74] Bucciantini, M.; Giannoni, E.; Chiti, F.; Baroni, F.; Formigli, L.; Zurdo, J.; Taddei, N.; Ramponi, G.; Dobson, C.M.; Stefani, M. Inherent toxicity of aggregates implies a common mechanism for protein misfolding diseases. *Nature*, **2002**, *416*(6880), 507-511.

[75] Macario, A.J.; Conway de Macario, E. Chaperonopathies and chaperonotherapy. *FEBS Lett.*, **2007**, *581*(19), 3681-3688.

[76] Schenk, D.; Barbour, R.; Dunn, W.; Gordon, G.; Grajeda, H.; Guido, T.; Hu, K.; Huang, J.; Johnson-Wood, K.; Khan, K.; Kholodenko, D.; Lee, M.; Liao, Z.; Lieberburg, I.; Motter, R.; Mutter, L.; Soriano, F.; Shopp, G.; Vasquez, N.; Vandevert, C.; Walker, S.; Wogulis, M.; Yednock, T.; Games, D.; Seubert, P. Immunization with amyloid-beta attenuates Alzheimer-disease-like pathology in the PDAPP mouse. *Nature*, **1999**, *400*(6740), 173-177.

[77] Janus, C.; Pearson, J.; McLaurin, J.; Mathews, P.M.; Jiang, Y.; Schmidt, S.D.; Chishti, M.A.; Horne, P.; Heslin, D.; French, J.; Mount, H.T.; Nixon, R.A.; Mercken, M.; Bergeron, C.; Fraser, P.E.; St George-Hyslop, P.; Westaway, D. A beta peptide immunization reduces behavioural impairment and plaques in a model of Alzheimer's disease. *Nature*, **2000**, *408*(6815), 979-982.

[78] Glabe, C.G. Structural classification of toxic amyloid oligomers. *J. Biol. Chem.*, **2008**, *283*(44), 29639-29643.

[79] Sharon, R.; Bar-Joseph, I.; Frosch, M.P.; Walsh, D.M.; Hamilton, J.A.; Selkoe, D.J. The formation of highly soluble oligomers of alpha-synuclein is regulated by fatty acids and enhanced in Parkinson's disease. *Neuron*, **2003**, *37*(4), 583-595.

[80] Arawaka, S.; Wada, M.; Goto, S.; Karube, H.; Sakamoto, M.; Ren, C.H.; Koyama, S.; Nagasawa, H.; Kimura, H.; Kawanami, T.; Kurita, K.; Tajima, K.; Daimon, M.; Baba, M.; Kido, T.; Saino, S.; Goto, K.; Asao, H.; Kitanaka, C.; Takashita, E.; Hongo, S.; Nakamura, T.; Kayama, T.; Suzuki, Y.; Kobayashi, K.; Katagiri, T.; Kurokawa, K.; Kurimura, M.; Toyoshima, I.; Niizato, K.; Tsuchiya, K.; Iwatsubo, T.; Muramatsu, M.; Matsumine, H.; Kato, T. The role of G-protein-coupled receptor kinase 5 in pathogenesis of sporadic Parkinson's disease. *J. Neurosci.*, **2006**, *26*(36), 9227-9238.

[81] Karube, H.; Sakamoto, M.; Arawaka, S.; Hara, S.; Sato, H.; Ren, C.H.; Goto, S.; Koyama, S.; Wada, M.; Kawanami, T.; Kurita, K.; Kato, T. N-terminal region of alpha-synuclein is essential for the fatty acid-induced oligomerization of the molecules. *FEBS Lett.*, **2008**, *582*(25-26), 3693-3700.

[82] Wang, J.; Farr, G.W.; Zeiss, C.J.; Rodriguez-Gil, D.J.; Wilson, J.H.; Furtak, K.; Rutkowski, D.T.; Kaufman, R.J.; Ruse, C.I.; Yates, J.R., 3rd; Perrin, S.; Feany, M.B.; Horwich, A.L. Progressive aggregation despite chaperone associations of a mutant SOD1-YFP in transgenic mice that develop ALS. *Proc. Natl. Acad. Sci. USA*, **2009**, *106*(5), 1392-1397.

[83] Arai, T.; Hasegawa, M.; Akiyama, H.; Ikeda, K.; Nonaka, T.; Mori, H.; Mann, D.; Tsuchiya, K.; Yoshida, M.; Hashizume, Y.; Oda, T. TDP-43 is a component of ubiquitin-positive tau-negative inclusions in frontotemporal lobar degeneration and amyotrophic lateral sclerosis. *Biochem. Biophys. Res. Commun.*, **2006**, *351*(3), 602-611.

[84] Neumann, M.; Sampathu, D.M.; Kwong, L.K.; Truax, A.C.; Micsenyi, M.C.; Chou, T.T.; Bruce, J.; Schuck, T.; Grossman, M.; Clark, C.M.; McCluskey, L.F.; Miller, B.L.; Masliah, E.; Mackenzie, I.R.; Feldman, H.; Feiden, W.; Kretzschmar, H.A.; Trojanowski, J.Q.; Lee, V.M. Ubiquitinated TDP-43 in frontotemporal lobar degeneration and amyotrophic lateral sclerosis. *Science*, **2006**, *314*(5796), 130-133.

[85] Kabashi, E.; Valdmanis, P.N.; Dion, P.; Spiegelman, D.; McConkey, B.J.; Vande Velde, C.; Bouchard, J.P.; Lacomblez, L.; Pochigaeva, K.; Salachas, F.; Pradat, P.F.; Camu, W.; Meininger, V.; Dupre, N.; Rouleau, G.A. TARDBP mutations in individuals with sporadic and familial amyotrophic lateral sclerosis. *Nat. Genet.*, **2008**, *40*(5), 572-574.

[86] Gitcho, M.A.; Baloh, R.H.; Chakraverty, S.; Mayo, K.; Norton, J.B.; Levitch, D.; Hatanpaa, K.J.; White, C.L., 3rd; Bigio, E.H.; Caselli, R.; Baker, M.; Al-Lozi, M.T.; Morris, J.C.; Pestronk, A.; Rademakers, R.; Goate, A.M.; Cairns, N.J. TDP-43 A315T mutation in familial motor neuron disease. *Ann. Neurol.*, **2008**, *63*(4), 535-538.

[87] Sreedharan, J.; Blair, I.P.; Tripathi, V.B.; Hu, X.; Vance, C.; Rogelj, B.; Ackerley, S.; Durnall, J.C.; Williams, K.L.; Buratti, E.; Baralle, F.; de Belleroche, J.; Mitchell, J.D.; Leigh, P.N.; Al-Chalabi, A.; Miller, C.C.; Nicholson, G.; Shaw, C.E. TDP-43 mutations in familial and sporadic amyotrophic lateral sclerosis. *Science*, **2008**, *319*(5870), 1668-1672.

[88] Yokoseki, A.; Shiga, A.; Tan, C.F.; Tagawa, A.; Kaneko, H.; Koyama, A.; Eguchi, H.; Tsujino, A.; Ikeuchi, T.; Kakita, A.; Okamoto, K.; Nishizawa, M.; Takahashi, H.; Onodera, O. TDP-43 mutation in familial amyotrophic lateral sclerosis. *Ann. Neurol.*, **2008**, *63*(4), 538-542.

[89] Kalmar, B.; Greensmith, L. Induction of heat shock proteins for protection against oxidative stress. *Adv. Drug Deliv. Rev.*, **2009**, *61*(4), 310-318.

[90] Cuervo, A.M.; Stefanis, L.; Fredenburg, R.; Lansbury, P.T.; Sulzer, D. Impaired degradation of mutant alpha-synuclein by chaperone-mediated autophagy. *Science*, **2004**, *305*(5688), 1292-1295.

[91] Dickey, C.A.; Kamal, A.; Lundgren, K.; Klosak, N.; Bailey, R.M.; Dunmore, J.; Ash, P.; Shoraka, S.; Zlatkovic, J.; Eckman, C.B.; Patterson, C.; Dickson, D.W.; Nahman, N.S., Jr.; Hutton, M.; Burrows, F.; Petrucelli, L. The high-affinity HSP90-CHIP complex recognizes and selectively degrades phosphorylated tau client proteins. *J. Clin. Invest.*, **2007**, *117*(3), 648-658.

[92] Goryunov, D.; Liem, R.K. CHIP-ping away at tau. *J. Clin. Invest.*, **2007**, *117*(3), 590-592.

[93] Sherman, M.Y.; Goldberg, A.L. Cellular defenses against unfolded proteins: a cell biologist thinks about neurodegenerative diseases. *Neuron*, **2001**, *29*(1), 15-32.

[94] Calderwood, S.K.; Mambula, S.S.; Gray, P.J., Jr.; Theriault, J.R. Extracellular heat shock proteins in cell signaling. *FEBS Lett.*, **2007**, *581*(19), 3689-3694.

[95] van Noort, J.M. Stress proteins in CNS inflammation. *J. Pathol.*, **2008**, *214*(2), 267-275.

Received: July 03, 2009 **Revised: October 30, 2009** **Accepted: November 09, 2009**

THE JOURNAL OF BIOLOGICAL CHEMISTRY VOL. 285, NO. 52, pp. 40732–40744, December 24, 2010

Phosphorylated α-Synuclein at Ser-129 Is Targeted to the Proteasome Pathway in a Ubiquitin-independent Manner*

Received for publication, May 7, 2010, and in revised form, September 22, 2010 Published, JBC Papers in Press, October 19, 2010, DOI 10.1074/jbc.M110.141952

Youhei Machiya[1], Susumu Hara[1], Shigeki Arawaka[2], Shingo Fukushima, Hiroyasu Sato, Masahiro Sakamoto, Shingo Koyama, and Takeo Kato

From the Department of Neurology, Hematology, Metabolism, Endocrinology, and Diabetology, Faculty of Medicine, Yamagata University, Yamagata 990-9585, Japan

α-Synuclein (a-Syn) is a major component of fibrillar aggregates in Lewy bodies (LBs), a characteristic hallmark of Parkinson disease. Almost 90% of a-Syn deposited in LBs is phosphorylated at Ser-129. However, the role of Ser-129-phosphorylated a-Syn in the biogenesis of LBs remains unclear. Here, we investigated the metabolism of Ser-129-phosphorylated a-Syn. In SH-SY5Y cells, inhibition of protein phosphatase 2A/1 by okadaic acid, and inhibition of the proteasome pathway by MG132 or lactacystin accumulated Ser-129-phosphorylated a-Syn. However, these inhibitions did not alter the amounts of total a-Syn within the observation time. Inhibition of the autophagy-lysosome pathway by 3-methyladenine or chloroquine accumulated Ser-129-phosphorylated a-Syn in parallel to total a-Syn during longer incubations. Experiments using cycloheximide showed that Ser-129-phosphorylated a-Syn diminished rapidly ($t_{½}$ = 54.9 ± 6.4 min), in contrast to the stably expressed total a-Syn. The short half-life of Ser-129-phosphorylated a-Syn was blocked by MG132 to a greater extent than okadaic acid. In rat primary cortical neurons, either MG132, lactacystin, or okadaic acid accumulated Ser-129-phosphorylated a-Syn. Additionally, we did not find that phosphorylated a-Syn was ubiquitinated in the presence of proteasome inhibitors. These data show that Ser-129-phosphorylated a-Syn is targeted to the proteasome pathway in a ubiquitin-independent manner, in addition to undergoing dephosphorylation. The proteasome pathway may play a role in the biogenesis of Ser-129-phosphorylated a-Syn-rich LBs.

Sporadic Parkinson disease (sPD)[3] is characterized pathologically by a loss of dopaminergic neurons in the substantia nigra pars compacta and the presence of intracytoplasmic inclusions called Lewy bodies (LBs) and Lewy neurites (LNs) in surviving neurons. α-Synuclein (a-Syn) is a major component of fibrillar aggregates in LBs and LNs. Accumulating lines of evidence have shown that prefibrillar intermediates of a-Syn, such as soluble oligomers or protofibrils, play a toxic role in degeneration of dopaminergic neurons, and mature fibrils of a-Syn contribute toward this toxicity to a lesser extent (1–4). Therefore, the process of a-Syn aggregation eventually forming LBs is proposed to play a causative role in neuronal degeneration of PD (5, 6). Immunohistochemical and biochemical studies have revealed that ~90% of a-Syn deposited in LBs is phosphorylated at serine 129 (Ser-129) (7, 8). In contrast, the portion of phosphorylated a-Syn in normal brains is known to be only about 4% (7) or less than the limits of quantification of the assays used (8). This discrepancy implicates a pathogenic role of Ser-129-phosphorylated a-Syn in the biogenesis of LBs (7, 9). One possibility is that the Ser-129-phosphorylation promotes the aggregation-prone property of a-Syn. To elucidate this issue, several *in vitro* studies have been performed. However, the accelerating effect of phosphorylation on fibril formation of a-Syn is controversial at present (7, 10). Another possibility is that the impairment of the system to degrade Ser-129-phosphorylated a-Syn causes its accumulation. However, the process by which Ser-129-phosphorylated a-Syn is degraded or recycled remains unknown. This study focused on the metabolic fate of Ser-129-phosphorylated a-Syn in cells. We report here that Ser-129-phosphorylated a-Syn undergoes dephosphorylation and degradation by the proteasome pathway. In addition, Ser-129-phosphorylated a-Syn is targeted to the proteasome pathway in a ubiquitin-independent manner.

EXPERIMENTAL PROCEDURES

Plasmid cDNA Construction and Reagents—Wild-type human a-Syn cDNA was described previously (11). S129A, S129E, S129D mutant a-Syn cDNAs were made by the two step PCR mutagenesis method. S9A/S42A/S87A mutant (it abolished Ser residues other than Ser-129) and K12R/K21R/K23R mutant a-Syn cDNAs (it abolished Lys residues for ubiquitination) (8) were generated by applying the two-step PCR mutagenesis method. Human ubiquitin cDNAs with or without a FLAG tag at the N terminus were generated by PCR (clone ID 3879581; Open Biosystems, Huntsville, AL), and they were subcloned into the pcDNA3.1 vector (Invitrogen, Carlsbad, CA). Nucleotide sequences of all constructs were confirmed by direct sequencing. All reagents were purchased from Sigma unless otherwise stated.

Cell Culture and Transfection—Human dopaminergic neuroblastoma SH-SY5Y cells (ECACC 94030304) were maintained in a mixture of F-12 and Eagle's minimum essential medium supplemented with 15% fetal bovine serum (Invitrogen), 1× non-essential amino acids, and 2 mM L-glutamine

* This work was supported in part by a Grant-in-Aid from the Global COE Program (F03) of the Japan Society for the Promotion of Science (to T. K.).
[1] Both authors contributed equally to this work.
[2] To whom correspondence should be addressed: 2-2-2 Iida-nishi, Yamagata 990-9585, Japan. Fax: 81-23-628-5318; E-mail: arawaka@med.id.yamagata-u.ac.jp.
[3] The abbreviations used are: sPD, sporadic Parkinson disease; CHX, cycloheximide; a-Syn, α-synuclein; OA, okadaic acid; 3-MA, 3-methyladenine.

(Invitrogen) at 37 °C in 5% CO_2. The SH-SY5Y cell line stably expressing wild-type a-Syn (wt-aS/SH) was selected against with 1 mg/ml G418 (Invitrogen). For transient transfection, 5×10^6 cells were transfected with 6 μg of cDNA using Nucleofector (Amaxa Cell Line Nucleofector kit V; Lonza Cologne AG, Koln, Germany). The cells were harvested at 48 h post-transfection.

Primary Neuronal Cultures—Primary cortical neuron cultures were prepared from Crl:CD (SD) rats as previously described (11). Briefly, neurons were isolated from the neocortex of embryonic day 18 rats and dissociated cells were plated at a density of 1×10^6 cells on poly-D-lysine-coated 6-well plates (Becton Dickinson, Bedford, MA). Neurons were maintained in serum-free medium, which was composed of neurobasal medium supplemented with B27 and GlutaMAX (Invitrogen). At intervals of 2 days, half of the plating medium was renewed. At 21 days of culture, neurons were harvested for experiments (12).

Chemical Treatments—For inhibition of the proteasome, at 16 h after plating wt-aS/SH cells onto 6-well plates, we checked the cells to be ~80% confluent, and then the cells were further incubated in fresh medium containing either 10 nM okadaic acid (OA), 10 μM MG132, or 10 μM lactacystin for 4 h. As a vehicle control, cells were treated with the same concentration of DMSO, which was used for dissolving OA, MG132, and lactacystin, or phosphate buffered saline (PBS: 1.06 mM KH_2PO_4, 2.97 mM $Na_2HPO_4 \cdot 7H_2O$, 150 mM NaCl). In rat primary neuronal cultures, neurons were cultured for 21 days and then incubated in fresh medium containing either 10 nM OA, 10 μM MG132, or 10 μM lactacystin for 4 h. For inhibition of the autophagy-lysosome, at 16 h post-plating wt-aS/SH cells onto 6-well plates, we confirmed the cells to be around 50% confluent. The cells were incubated in fresh medium containing 10 mM 3-metyladenine (3-MA) or 100 μM chloroquine for up to 32 h.

To assess protein half-lives in the cells, we performed experiments using the *de novo* protein synthesis inhibitor, cycloheximide (CHX). At 16 h post-plating wt-aS/SH cells onto 6-well plates, we confirmed the cells to be ~80% confluent. The cells were incubated in fresh medium containing 100 μM CHX for the indicated times. To test the effect of inhibition of the proteasome pathway or dephosphorylation on the half-lives of target proteins, we treated the cells with CHX plus either MG132 or OA. The 80% confluent wt-aS/SH cells were pre-incubated in fresh medium containing either DMSO, 10 μM MG132, or 10 nM OA for 6 h. After preincubation, CHX was added to a final concentration of 100 μM into medium. The cells were further incubated for the indicated times.

Protein Extract Preparation—For preparation of cell lysates, SH-SY5Y cells were suspended in buffer A (20 mM Tris-HCl, pH 7.4, 150 mM NaCl, 1% Nonidet P-40, 10% glycerol, 1 × protease inhibitor mixture (Roche Diagnostic, Mannheim, Germany), 1 mM EDTA, 1 × phosSTOP (Roche Diagnostic)) and kept on ice for 30 min. After centrifugation at 12,000 × *g* for 30 min, the resultant supernatant was collected and stored at −80 °C until required. In primary neuronal cultures, the cells were suspended in buffer A containing 1 μM OA, and then they were disrupted by passing through a 27-gauge needle 10 times.

In the experiments for ubiquitinated proteins, the pellet from above (post-12,000 × *g* centrifugation step) was resuspended in the same aliquots of buffer A containing 8 M urea and was disrupted by brief sonication. After centrifugation at 12,000 × *g* for 30 min, the resultant supernatant was collected as the pellet fraction. The protein concentration was measured by the BCA assay (Thermo Scientific, Rockford, IL).

Immunoprecipitation—The cells were suspended in ice-cold lysis buffer (20 mM Tris-HCl, pH 7.4, 150 mM NaCl, 1% Triton X-100, 0.1% SDS, 0.5% deoxycholic acid, 10% glycerol, 1× protease inhibitor mixture, 1 mM EDTA, 20 mM NaF, 1 mM Na_3VO_4, 1 μM OA), and kept on ice for 30 min. After centrifugation at 12,000 × *g* for 30 min, the resultant supernatant was collected. The supernatants were incubated with primary antibodies overnight at 4 °C, and then incubated with Protein G-agarose beads for 2 h. Beads were washed three times with ice-cold lysis buffer, and immunoprecipitates were dissolved from the beads by heating in Laemmli's sample buffer. Equivalent amounts of samples were analyzed by immunoblotting.

Immunoblotting—For SDS-PAGE, protein samples were denatured at 95 °C for 5 min in Laemmli's sample buffer containing 2.5% 2-mercaptoethanol. Samples were applied to a 12.5% SDS-polyacrylamide gel, electrophoresed and then transferred to a PVDF membrane (Millipore, Billerica, MA). After blocking with 5% skim milk in Tris-buffered saline (pH 7.4) containing 0.05% Tween-20 (TBS-T) for 1 h at room temperature, the membrane was incubated with primary antibodies overnight at 4 °C followed by incubation with horseradish peroxidase-conjugated secondary antibodies (Jackson ImmunoResearch Lab., Inc., West Grove, PA) for 1 h at room temperature or overnight at 4 °C. The membrane was reacted with ECL (GE Healthcare, Uppsala, Sweden) for the detection of β-actin, G-protein-coupled receptor kinase (GRK) 2, and total a-Syn, including phosphorylated and non-phosphorylated forms, or ECL plus (GE Healthcare) for the detection of other proteins. The membrane was then visualized using a CCD camera, VersaDog 5000 (Bio-Rad). Relative intensities of detected signals were quantified with Quantity one software (Bio-Rad). For detection of phosphorylated a-Syn, we added 50 mM NaF into TBS-T containing 5% milk or antibodies.

The following primary antibodies were used (11, 13): monoclonal anti-a-Syn antibody (Syn-1, it recognizes total a-Syn including phosphorylated and non-phosphorylated forms, 1:4,000; BD Transduction Laboratories, Franklin Lakes, NJ), monoclonal anti-Ser-129-phosphorylated a-Syn antibody (psyn 64, 1:5,000; Wako, Osaka, Japan), monoclonal anti-β-actin antibody (AC-15, 1:10,000; Sigma), polyclonal anti-GRK2 antibody (sc-562, 1:1,000; Santa Cruz Biotechnology, Santa Cruz, CA), polyclonal anti-GRK3 antibody (sc-563, 1:1,000; Santa Cruz Biotechnology), monoclonal anti-GRK5 antibody (139, 1:5,000) (13), polyclonal anti-GRK6 antibody (sc-566, 1:1,000; Santa Cruz Biotechnology), polyclonal anti-casein kinase (CK) 2α′ antibody (sc-648, 1:1,000; Santa Cruz Biotechnology), and polyclonal anti-ubiquitin antibody (1:1,000, Dako, Glostrup, Denmark).

Quantification of Band Intensities—In experiments for estimating the protein half-lives, we quantified the relative band intensities of phosphorylated or total a-Syn by using protein standards. Recombinant non-phosphorylated a-Syn proteins were purified from *Escherichia coli* as described previously (14). Phosphorylated a-Syn proteins were made by incubation of 100 μg of non-phosphorylated proteins in reaction buffer (20 mM Tris-HCl, pH 7.5, 50 mM KCl, 10 mM $MgCl_2$, 200 μM ATP) containing 1,000 units of recombinant CK2 protein (New England Biolabs, Beverly, MA) for 16 h at 37 °C. A set of diluted non-phosphorylated or phosphorylated a-Syn proteins was subjected to SDS-PAGE along with samples. After quantifying band intensities of samples with Quantity one software, they were plotted on a standard curve and corrected relative intensities. Statistical comparisons were made by unpaired Student's *t* test.

Pulse-chase Metabolic Labeling Experiments—Wt-aS/SH cells were rinsed with PBS and incubated with methionine/cystine-free medium for 1 h. The cells were pulsed with methionine/cystine-free medium containing 100 μCi/ml of [^{35}S]methionine/cysteine (PerkinElmer Life Sciences) for 2 h, and subsequently chased with normal medium containing 1 mM methionine and cysteine for indicated times. After harvesting cells, immunoprecipitation using Syn-1 antibody or anti-Ser-129-phosphorylated a-Syn antibody was carried out. Immunoprecipitates were subjected to 12.5% gels and transferred to the PVDF membrane. Signals were detected by BAS-2000 image analyzer (Fuji Photo Film Co.).

Immunocytochemistry—Wt-aS/SH cells transfected with ubiquitin cDNA were plated on 4-chamber slides (Nunc, Rochester, NY) at 1×10^5 cells per well. After 2 days, the cells were incubated with medium containing either DMSO, 10 μM MG132, or 10 nM OA for 16 h, fixed with 4% paraformaldehyde for 15 min at room temperature and incubated with PBS containing 0.2% Triton X-100 for 5 min. After blocking with 5% skim milk, they were labeled with anti-a-Syn monoclonal antibody (LB509, 1:250; Covance, Emeryville, CA) and anti-ubiquitin polyclonal antibody (1:50) overnight at 4 °C. Then, the cells were incubated with Alexa Fluor 488 anti-mouse IgG and Alexa Fluor 568 anti-rabbit IgG (Invitrogen) for 2 h at 37C°. The slides were analyzed with a LSM510 meta laser confocal microscope (Zeiss, Jena, Germany).

RESULTS

The Effect of Protein Phosphatase 2A/1 Inhibitor on the Levels of Ser-129-phosphorylated a-Syn in SH-SY5Y Cells—The metabolic fate of a phosphorylated protein is affected by dephosphorylation and/or degradation pathways, such as the proteasome or autophagy-lysosome pathway. Fujiwara *et al.* (7) has reported that Ser-129-phosphorylated a-Syn protein underwent dephosphorylation. This idea is supported by the findings showing that the protein phosphatase 2A/1 inhibitor, OA, increases the amount of phosphorylated a-Syn in PC12 cells (15) and HEK293 cells (11). To compare the contribution of dephosphorylation to the metabolism of Ser-129-phosphorylated a-Syn with that of degradation pathways, we first assessed the effect of OA on the metabolism of Ser-129-phosphorylated a-Syn. In this study, we used a cell line (wt-aS/SH) stably expressing wild-type a-Syn, because it is difficult to detect Ser-129-phosphorylated a-Syn at endogenous levels in SH-SY5Y cells. As compared with the starting levels, the expression levels of Ser-129-phosphorylated a-Syn were increased 2.60 ± 0.43-fold at 2 h (mean ± S.D., $p < 0.01$, $n = 4$) and 5.53 ± 2.32-fold at 4 h ($p = 0.03$, $n = 4$) in the presence of 10 nM OA (Fig. 1). In contrast, the expression levels of total a-Syn, including non-phosphorylated and phosphorylated forms, were constant at 0.92 ± 0.04-fold at 2 h ($p = 0.125$, $n = 3$) and 1.03 ± 0.23-fold at 4 h ($p = 0.861$, $n = 3$), when compared with starting levels (Fig. 1). Unexpectedly, the expression levels of Ser-129-phosphorylated a-Syn were moderately but significantly increased 1.82 ± 0.44-fold at 4 h in the presence of 0.1% DMSO ($p = 0.014$, $n = 5$) (Fig. 1). When the cells were incubated in medium containing 0.1% PBS for 4 h, the levels of Ser-129-phosphorylated a-Syn were constant (Fig. 1). The increased effect of OA on the levels of phosphorylated a-Syn was larger than that of DMSO at 4 h of post-treatment (5.53 ± 2.32-fold in OA *versus* 1.82 ± 0.44-fold in DMSO) (Fig. 1).

The Effect of Proteasome Inhibitors on the Levels of Ser-129-phosphorylated a-Syn in SH-SY5Y Cells—We tested whether Ser-129-phosphorylated a-Syn was degraded by the proteasome pathway, because phosphorylation sometimes acts as a signal to target the proteins, such as IκBα (16) and β-catenin (17), to the ubiquitin-proteasome pathway. We treated wt-aS/SH cells with the proteasome inhibitor, MG132, for 4 h. The expression levels of Ser-129-phosphorylated a-Syn were increased 5.07 ± 1.86-fold at 2 h ($p = 0.022$, $n = 4$) and 10.6 ± 5.46-fold at 4 h ($p = 0.039$, $n = 4$), as compared with the starting levels (Fig. 2). Treatment with another proteasome inhibitor, lactacystin, also showed a 15.3 ± 8.24-fold increase in the levels of Ser-129-phosphorylated a-Syn at 4 h ($p = 0.04$, $n = 4$) (Fig. 2). In contrast, the expression levels of total a-Syn were constant at 1.00 ± 0.08-fold in MG132 ($p = 0.929$, $n = 4$) and 1.00 ± 0.14-fold in lactacystin ($p = 0.986$, $n = 4$) at 4 h (Fig. 2). The increased effect of proteasome inhibitors on the levels of phosphorylated a-Syn was much larger than that of DMSO at 4 h post-treatment (15.3 ± 8.24-fold in lactacystin *versus* 1.82 ± 0.44-fold in DMSO) (Fig. 2).

The Effect of Autophagy-Lysosome Inhibitors on the Levels of Ser-129-phosphorylated a-Syn in SH-SY5Y Cells—We next tested whether Ser-129-phosphorylated a-Syn was degraded by the autophagy-lysosome pathway. As compared with the starting levels, the expression levels of Ser-129-phosphorylated a-Syn were increased 2.05 ± 0.52-fold at 32 h in the presence of 10 mM 3-MA, which inhibits the formation of the autophagosome ($p = 0.027$, $n = 3$) (Fig. 3). The expression levels of total a-Syn were also increased 1.5 ± 0.06-fold at 32 h ($p = 0.005$, $n = 3$) (Fig. 3). Additionally, treatment with 100 μM of general lysosomal inhibitor, chloroquine, showed that the expression levels of Ser-129-phosphorylated a-Syn were 6.52 ± 2.20-fold higher than the starting levels at 32 h ($p = 0.049$, $n = 3$) (Fig. 3). The expression levels of total a-Syn were found to be increased 1.39 ± 0.10-fold at 32 h ($p = 0.022$, $n = 3$) (Fig. 3). When the cells were treated with 0.1% PBS as a vehicle control, the levels of Ser-129-phosphorylated and total a-Syn were constant. Inhibition of the autophagy-

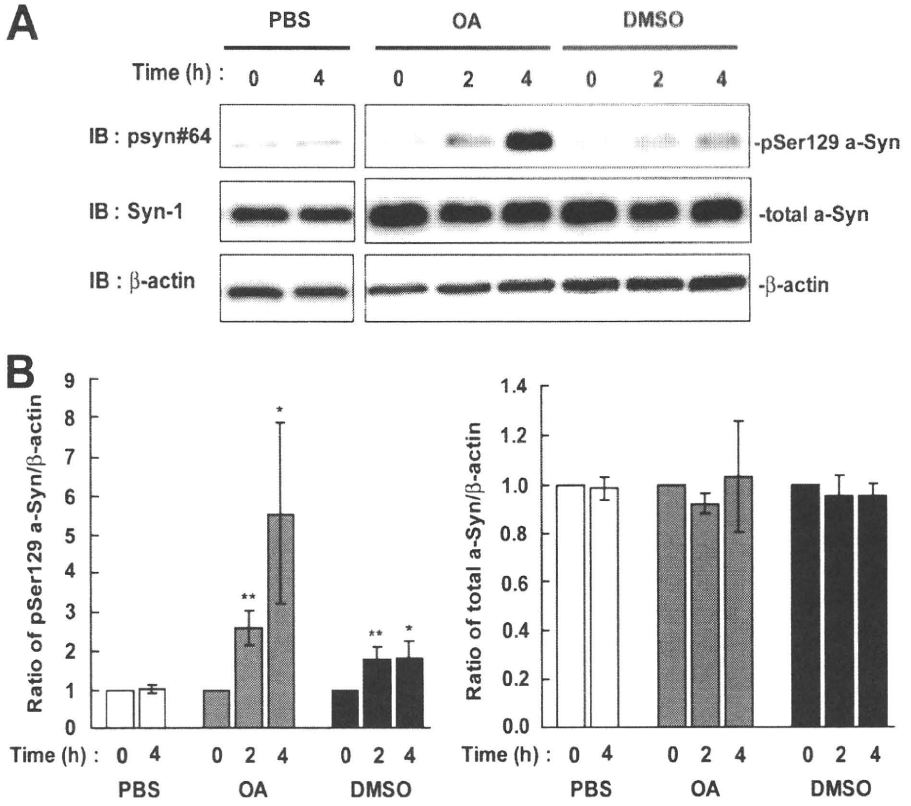

FIGURE 1. **The effect of protein phosphatase 2A/1 inhibitor on the levels of Ser-129-phosphorylated a-Syn in SH-SY5Y cells.** SH-SY5Y cells stably expressing wild-type a-Syn (*wt-aS/SH*) were incubated in medium containing either 0.1% PBS, 0.1% DMSO or 10 nM OA for 4 h. *A*, cell lysates (20 μg/lane) were loaded on SDS-PAGE and analyzed by immunoblotting (*IB*) with anti-Ser-129-phosphorylated a-Syn antibody (*psyn 64*) and anti-total a-Syn antibody (*Syn-1*). For loading control, the same amounts of samples were immunoblotted with anti-β-actin antibody. Representative blots are shown. *B*, quantitative analysis of the alteration in the expression levels of Ser-129-phosphorylated a-Syn in cells in the absence or presence of OA. Relative ratios of the band intensity of Ser-129-phosphorylated a-Syn to β-actin and total a-Syn to β-actin are shown. Relative ratio was normalized to the starting material just before adding reagents. Data represent means ± S.D. and the *p* values (*, $p < 0.05$; **, $p < 0.01$) were estimated by unpaired Student's *t* test.

lysosome pathway showed that the expression levels of Ser-129-phosphorylated a-Syn were elevated almost in parallel to those of total a-Syn by longer incubations than inhibition of the proteasome pathway.

Role of Dephosphorylation and Proteasomal Degradation in the Metabolism of Ser-129-phosphorylated a-Syn in SH-SY5Y Cells—To elucidate the contribution of dephosphorylation and degradation pathways to the metabolism of Ser-129-phosphorylated a-Syn, we determined the half-life of Ser-129-phosphorylated a-Syn by using the *de novo* protein synthesis inhibitor, CHX, in wt-aS/SH cells. As shown in Fig. 4, *A* and *B*, the experiment using CHX showed that the amounts of Ser-129-phosphorylated a-Syn were rapidly decreased. Its estimated half-life ($t_{1/2}$) was 54.9 ± 6.4 min. In contrast, the expression levels of total a-Syn were stable within the observation time of up to 240 min (Fig. 4, *A* and *B*). Because this finding suggested that Ser-129-phosphorylated a-Syn was rapidly processed by the specific pathway that differed from the non-phosphorylated form, we then focused on the role of dephosphorylation and degradation by the proteasome pathway. We treated wt-aS/SH cells with CHX plus either OA or MG132. To ensure that OA or MG132 exerts its inhibitory effect during the entire course of the experiment, we pretreated the cells with the reagents until accumulation of Ser-129-phosphorylated a-Syn was easily detectable. Under these conditions, treatment with OA suppressed the decrease in the amounts of Ser-129-phosphorylated a-Syn (Fig. 4, *A* and *B*). The amounts of Ser-129-phosphorylated a-Syn were decreased to about 50% at 240 min in the presence of OA (Fig. 4, *A* and *B*). Treatment with MG132 remarkably blocked the decrease in the amounts of Ser-129-phosphorylated a-Syn (Fig. 4, *A* and *B*). The amounts of Ser-129-phosphorylated a-Syn were almost constant in the presence of MG132 (Fig. 4, *A* and *B*). The amounts of total a-Syn did not change in the presence of OA or MG132 (Fig. 4, *A* and *B*). These data suggested that Ser-129-phosphorylated a-Syn underwent degradation mainly by the proteasome pathway rather than dephosphorylation in SH-SY5Y cells. We performed pulse-chase experiments after metabolic labeling. Ser-129-phosphorylated a-Syn was decreased between 4 and 6 h of the chase periods, while total a-Syn was almost stable in the chase period (Fig. 4*C*). This finding was consistent with the data from experiments using CHX.

To exclude a possibility that the decrease in Ser-129-phosphorylated a-Syn was due to degradation of kinases, we examined whether treatment with CHX altered the expression levels of GRKs and CK2, which have been known to contribute to the Ser-129-phosphorylation of a-Syn (11, 13, 15, 18, 19). The expression levels of ubiquitously expressing members of GRKs (GRK2, -3, -5, and -6) and CK2 α′-subunit were stable in the presence of CHX and in the presence of CHX plus either OA or MG132 during the observation times (Fig. 4*D*).